

Photometric Observations of the Dwarf Nova AH Herculis

Corrado Spogli

Via Palazzolo 21 Frazione Spada 06020 Gubbio (PG), Italy; corradospogli@yahoo.it

Gianni Rocchi

Via Achille Grandi 14, 06038 Spello (PG), Italy; giannirocchi2@gmail.com

Stefano Ciprini

Space Science Data Center, Agenzia Spaziale Italiana (SSDC-ASI), I-00133, Roma, Italy, and Istituto Nazionale di Fisica Nucleare (INFN), Sezione di Roma Tor Vergata, I-00133, Roma, Italy; stefano.ciprini.asdc@gmail.com

Dario Vergari

Via Cantalmaggi 24, 06024 Gubbio (PG), Italy

Jacopo Rosati

Via XVIII Maggio N°4 06024 Gubbio (PG), Italy; jacopo.rosati@studenti.unipg.it

Received May 24, 2021; revised August 24, September 20, 2021; accepted September 20, 2021

Abstract We present the results of 274 nights of observations of the dwarf nova AH Herculis made in the years 2012, 2014, 2017, and 2018 for a total of 725 photometric data points. Observations were made in the B, V, R_c , and I_c Johnson-Cousins photometric bands. In 2012 AH Her was observed for 49 nights, in 2014 for 21 nights, and in 2017 and 2018 for 102 nights each year. Overall, we obtained 186 data points with the photometric filter B, 270 observations with the V filter, 165 with the R_c filter, and 104 with the I_c filter. The variable was well sampled in 2017 and 2018 and was observed on almost all clear nights; comments are missing in some filters due to technical problems with the filter wheel. The observations were all made at Gianni Rocchi's private observatory. In 2017 and 2018 we observed several outbursts of AH Her and in 2017 a standstill of short duration. In this work we present the observational data, the light curves obtained in 2012, 2017, and 2018, a study of the color indices, and the temporal characteristics of the outbursts of this dwarf nova.

1. Introduction

Cataclysmic variables (CVs) are binary stars containing a white dwarf that is accreting material from a red dwarf secondary or main sequence or subgiant companion (see Warner 1995 for a comprehensive review). An important subclass is the dwarf novae. Based on their photometric behavior, we distinguish a few subclasses of dwarf novae: U Gem, showing more or less similar outbursts; SU UMa, characterized by the so-called superoutbursts in addition to normal outbursts; Z Cam, with outbursts interrupted by irregular standstill (activity suspensions) intervals of constant brightness.

The U Gem variables have explosions that raise their brightness by 2 to 6 magnitudes and last for one or two days. In the following days the system returns to its usual brightness. SS Cyg variables are also called after their alternative prototype, SS Cygni, which periodically exhibits the brightest events of this subtype of variables.

The SU UMa sub-class is characterized by two very distinct outbursts types: short ones (lasting a few days) and superoutbursts which can last two weeks or longer in their rather bright “plateau” phase. Normal explosions are similar to those that occur in U Gem variables, while superoutbursts are two magnitudes brighter, last five times longer, and are three times less frequent. Typical superoutburst cycle lengths of these “ordinary” SU UMa stars range from 100 to 500 days. SU UMa systems generally have an orbital period $P_{\text{orb}} < 2$ hours

and brighter superoutbursts occurring every few months, while U Gem and Z Cam systems have $P_{\text{orb}} > 3$ hours and normal outbursts. Within the SU UMa class there is an additional distinction, from the most to the least active ones: ER UMa-type, pure SU UMa-type, and WZ Sge-type stars (see Hellier 2001 and Warner 2003 for a detailed overview). ER UMa stars have very short (much less than 100 d) regular supercycles, very short recurrence times of normal outbursts, and long duty cycles (for a review, see Kato *et al.* 1999) while WZ Sge-type dwarf novae are considered to be objects at the terminal stage of the cataclysmic variable (CV) evolution. WZ Sge stars are characterized by the large amplitude and long duration of superoutbursts which are accompanied by “early superhumps” in the early terms of the superoutbursts (see Kato 2015).

The main characteristics of the Z Cam subclass are: the short duration of minimum; the irregularity of the light curve, described as rare for U Gem types and almost the norm for Z Cams; the lesser amplitudes of variation compared to U Gems; and a “curious and very special feature” wherein the variable remains nearly constant at a magnitude in between the maximum and minimum: this peculiarity is called “standstill” and it is the most significant characteristic of assigning membership to the Z Cam classification of dwarf novae. The Z Cams are not very numerous; about 30 are known, and only 17 of the 19 bona fide Z Cams have orbital periods in the literature. All have periods from 3.048 hours (0.127 d) to 8.4 hours (0.38 d), the average being 5.272 hours (0.2196 d). Z Cams are very active systems.

Most have outburst cycles (the time between successive maxima) between 10 and 30 days. Their normal cycles between maxima and minima look very much like U Gem stars but they spend very little time at minimum.

Outburst amplitudes of Z Cam stars range from 2.3 to 4.9 magnitudes in V. The average amplitude is 3.7V magnitudes. This is identical to the range of amplitudes seen in U Gem stars, so it cannot be used to distinguish them from these more common dwarf novae. Z Cam systems that show “standstill” in their light curves are thought to be on the boundary between nova-like variable stars with their hot stable discs, and dwarf novae with their unstable discs (Smak 1983). The duration of standstills has a wide range, from tens of days to several years.

AH Her is a dwarf nova, Z Cam subtype, that varies in magnitude from $V=14.3$ in quiescence to $V=11.3$ during outburst, with outbursts lasting 4 to 18 days and recurring at intervals of 7 to 27 days (Ritter and Kolb 1998). AH Her is a very active dwarf nova. Spectroscopic observations were made by Williams (1983) that published a spectrum of the variable at minimum, giving the equivalent width of some lines of the Balmer series. Through spectroscopic observations, Horne *et al.* (1986) determined an orbital period for AH Her equal to $P=0.258116$ day (6.19 hours). They found a M2/M1 mass ratio of 0.80 with $M1 = 0.95$ and $M2 = 0.70$ solar masses; they calculated the inclination of the orbital plane and found $i = 46^\circ$ with respect to the secondary star of spectral type K. AH Her was detected in the ROSAT all-sky survey at a low rate (Verbunt *et al.* 1997). Simultaneous optical and UV (IUE) observations show that the UV flux follows the optical flux during an outburst (Verbunt *et al.* 1984). Wils *et al.* (2010) reports that the variable distance is 450 parsecs, while Ramsey *et al.* (2017), through Gaia satellite estimations, report a distance of this variable of 325.0 ± 47.2 parsecs. Further spectroscopic observations made by Echevarria *et al.* (2021), during a deep quiescent state, indicate that K5 is the most likely spectral type of the secondary and that the orbital period is $P = 0.25812 \pm 0.00032$ d, a value consistent with those determined by Horne *et al.* (1986).

Dwarf novae can have type A or type B outbursts. In type A with fast optical rise, the system brightens at longer wavelengths first, with shorter wavelengths delayed progressively. In type B with a slower rise, the rise is almost simultaneous at all wavelengths with at most only a small delay between optical and UV. This affects the light curve, which can be asymmetrical (type A) or symmetrical (type B). In a separate section we will deal with this issue and in the case of AH Her we will see that this dwarf nova can have both type A and type B outbursts.

2. Photometric observations and light curve

All the observations were obtained with a 0.12-m f/7 apochromatic refractor telescope by Skywatcher Esprit trademark, equipped with an Orion G3 CCD camera (Sony $I_c \times 419$ all), R_c , I_c Schuler filters, and U, B, V Baader filters. The exposure time was 240 sec. Our photometric system has been carefully tested by observing the M67 sequence (Chevalier and Ilovaisky 1991). The CCD frames were first corrected for de-biasing and flat fielding, then processed for aperture photometry. All the B, V, R_c data were obtained via differential photometry using the

photometric comparison stars 1, 2, 3 reported by Misselt (1996). To estimate the observations of AH Her made with the I_c filter we used the values $I_c(1) = 12.07 \pm 0.03$, $I_c(2) = 14.22 \pm 0.05$, $I_c(3) = 13.40 \pm 0.04$ reported by Spogli *et al.* (2001). Magnitude errors were evaluated as standard deviations of the mean. All observational data relating to the years 2012, 2014, 2017, and 2018 are shown in Appendix A after the references. A finding chart for AH Her is shown in Figure 1.

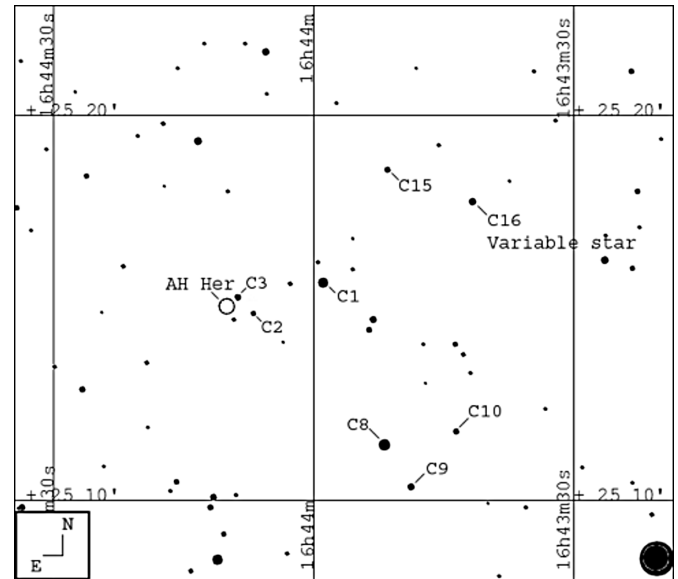


Figure 1. Finding chart for AH Her field.

2.1. Observations made in 2012

AH Her was observed sporadically in the V and R_c filters from 10 July 2012 to 7 November 2012 for a total of 49 nights, 42 of which were for observations in V and 7 in R_c . The star seems to maintain an average level of luminosity equal to $V=12.58 \pm 0.11$ magnitudes and $R_c = 12.56 \pm 0.13$ mag; however, the star oscillates in the V band between magnitude 12.88 and 12.31 and in the R_c band between 12.71 and 12.35, even if in the latter case the photometric data are few. In Figure 2 we present our light curve from 2012.

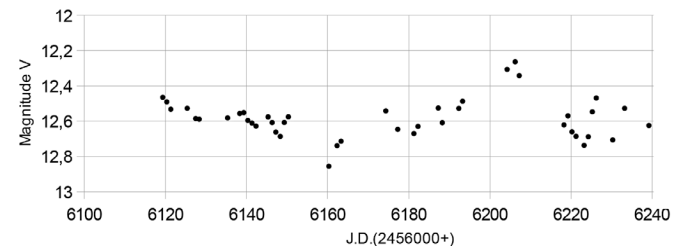


Figure 2. AH Her V band light curve in 2012.

2.2. Observations made in 2014

For the year 2014, we obtained sporadic observations in the four photometric filters: 5 observations in B, 18 in V, 9 in R_c , and 9 in I_c over a total of 21 nights. The low numbers of observations are due to technical problems at Gianni Rocchi’s telescope. We can, however, make a rough estimate of the color indices; at a minimum, the average color indices are:

$(B-V)=0.54\pm 0.08$, $(V-R)=0.49\pm 0.06$, $(V-I)=0.73\pm 0.14$, while in the phase of maximum light we only have a single estimate of the color index that is: $(B-V)=-0.02$.

2.3. Observations made in 2017

In 2017 AH Her was observed for 102 nights, from 22 April 2017 to 11 November 2017 in three photometric filters: B, V, R_c . There were few observations in the I_c filter due to technical problems with the filter wheel. The photometric data obtained were 314, divided as follows: 97 in B, 109 in V, 94 in R_c , and only 14 in I_c . Based on these data we have built the light curve in V that is presented in Figure 3, while in Figure 4 we present the light curve of AH Her in all four photometric filters.

From the analysis of the light curve of the variable in the V band, we can see that nine maximum brightnesses of AH Her and one standstill were observed.

The temporal distance between two consecutive maxima of the star is on average 20.5 days, while the duration of the standstill phase was almost 21 days. In Figure 5 we have represented the light curve of the variable during the standstill phase.

During the standstill, the average brightness values of AH Her in the different photometric bands were as follows: $B=12.6\pm 0.3$, $V=12.5\pm 0.2$, $R_c=12.3\pm 0.2$, and $I_c=12.1\pm 0.1$. After the standstill the star has a maximum brightness and it suggests that AH Her may belong to the IW And subclass of the Z Cam stars (Kato 2019).

Table 1 shows the main characteristics of our observational data for 2017.

2.4. Observations made in 2018

In 2018 AH Her was observed in four photometric filters; for three of the four filters data were obtained for 102 nights. We collected 331 photometric data divided as follows in the various filters: 84 data in B, 101 in V, 55 in R_c , and 81 in I_c . We occasionally had problems with the R_c filter, so we did not always manage to use it. In fact, in our observations there are missing data in particular from 02 July to 01 September 2018. Table 2 shows the main characteristics of our observational data for 2018. Figure 6 shows the light curve of AH Her in the V band for the year 2018, while Figure 7 shows the light curve of AH Her in all four photometric filters. Figure 8 shows the maximum brightness values reached during the various AH Her outbursts in 2018.

You may notice a slight decrease in brightness, and this is due to the worsening of the weather conditions in the months of October and November and to the fact that the outbursts were no longer observed continuously, hence the fragmented data. From a check of the observational data for October and November, the possible influence of the air mass on our observations does not emerge, since the variable at the time it was observed was high on above the horizon, and, also, the difference between the instrumental magnitudes of the comparison stars C1 and C3 always remained constant in the various observational bands and for the entire period of time in which AH Her was observed.

In Figure 9 we report the observational values of AH Her in B, V, and I_c , when the star was in the phase of minimum light. We can see an oscillating trend in the light curve.

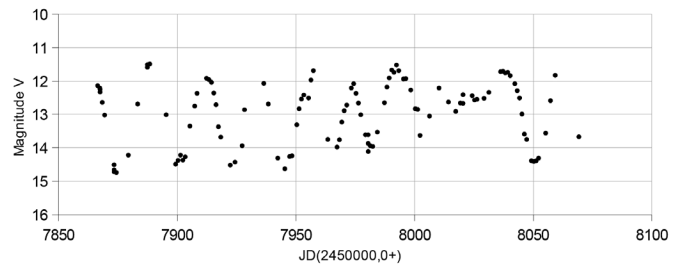


Figure 3. The V-band light curve of AH Her in 2017.

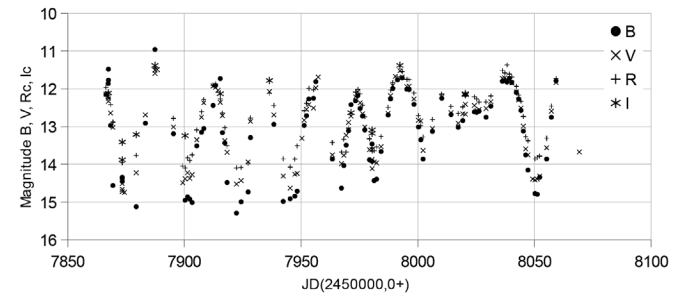


Figure 4. The 2017 light curve of AH Her in all four photometric filters (B, V, R_c , I_c).

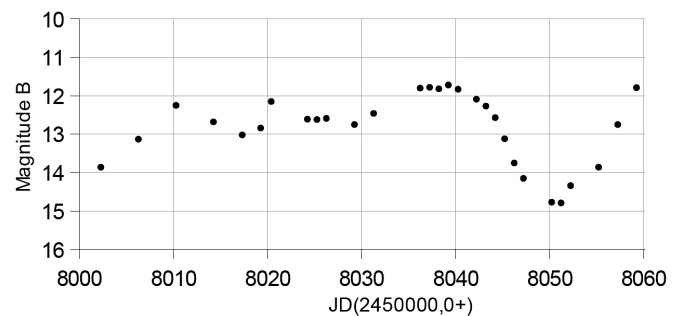


Figure 5. The light curve of AH Her during the standstill ranging from JD 2458010 to 2458030. Note that after the standstill phase, the variable has a new maximum and then a slow descent to the minimum brightness typical after a normal outburst.

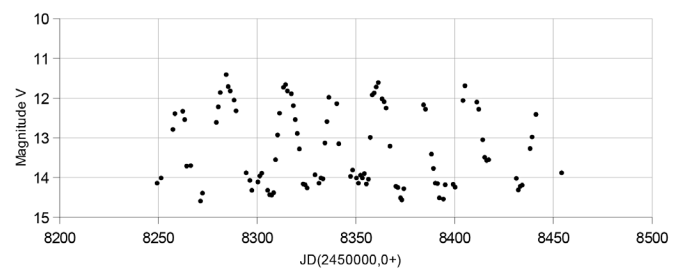


Figure 6. The V band light curve of AH Her in 2018; eight maximum brightness values corresponding to eight outbursts are clearly evident.

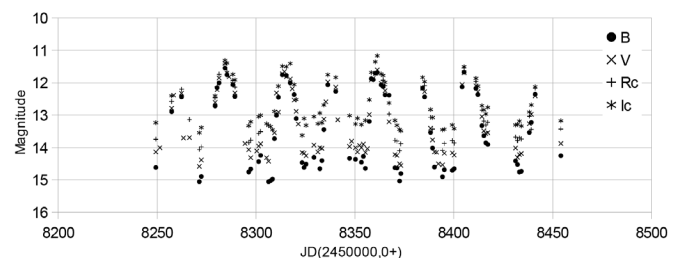


Figure 7. The 2018 light curve of AH Her in the four photometric bands (B, V, R_c , I_c).

Table 1. Summary data of AH Her 2017.

| | <i>B</i> | <i>B Error</i> | <i>V</i> | <i>V Error</i> | <i>R_c</i> | <i>R_c Error</i> | <i>I_c</i> | <i>I_c Error</i> |
|------------------------|----------|----------------|----------|----------------|----------------------|----------------------------|----------------------|----------------------------|
| Maximum Values | 10.96 | 0.04 | 11.49 | 0.05 | 11.37 | 0.03 | 11.38 | 0.03 |
| Minimum Values | 15.29 | 0.12 | 14.74 | 0.04 | 14.39 | 0.05 | 13.88 | 0.04 |
| Mean Values at Minimum | 14.66 | 0.31 | 14.25 | 0.30 | 13.78 | 0.25 | — | — |
| Mean Values at Maximum | 11.83 | 0.24 | 11.84 | 0.20 | 11.75 | 0.22 | — | — |

Table 2. Summary data of AH Her 2018.

| | <i>B</i> | <i>B Error</i> | <i>V</i> | <i>V Error</i> | <i>R_c</i> | <i>R_c Error</i> | <i>I_c</i> | <i>I_c Error</i> |
|------------------------|----------|----------------|----------|----------------|----------------------|----------------------------|----------------------|----------------------------|
| Maximum Values | 11.55 | 0.02 | 11.41 | 0.02 | 11.43 | 0.02 | 11.36 | 0.07 |
| Minimum Values | 15.06 | 0.02 | 14.56 | 0.03 | 14.09 | 0.02 | 13.63 | 0.11 |
| Mean Values at Minimum | 14.64 | 0.25 | 14.19 | 0.22 | 13.75 | 0.21 | 13.28 | 0.16 |
| Mean Values at Maximum | 11.89 | 0.19 | 11.87 | 0.19 | 11.84 | 0.22 | 11.66 | 0.24 |

Table 3. The mean values of color index in 2018. The errors on the color indices were calculated as standard deviation from the mean.

| | <i>B–V</i> | <i>B–V Error</i> | <i>V–R</i> | <i>V–R Error</i> | <i>R–I</i> | <i>R–I Error</i> | <i>V–I</i> | <i>V–I Error</i> |
|------------------------|------------|------------------|------------|------------------|------------|------------------|------------|------------------|
| Mean Values at Maximum | 0.04 | 0.05 | 0.11 | 0.06 | 0.12 | 0.08 | 0.28 | 0.10 |
| Mean values at Minimum | 0.45 | 0.11 | 0.43 | 0.09 | 0.51 | 0.09 | 0.93 | 0.14 |

Note: The errors on the color indices were calculated as standard deviation from the mean.

In Figure 10 we report the observed values of AH Her in *I_c* during the minimum light phase. We can see that the star oscillates between *I_c* magnitudes 13.6 and 12.9. The observational data relating to the star in the minimum luminous phase were selected by selecting a posteriori, from the analysis of the light curve, the days in which the star appeared faintly luminous.

3. A study of color indices

Bruch (1984) reported that the color index *B–V* varies from 0.04 to 0.13 in the maximum of an outburst, while in the minimum *B–V* varies from 0.24 to 0.55. In the years in which AH Her was better monitored, i.e. in 2017 and 2018, the color indices had different values depending on the state of the star. In 2017, in the first three outbursts observed, the *B–V* color index is strongly negative, as we can see from Figure 15, in which we have represented the color index *B–V* as a function of time, with values of *B–V* oscillating between -0.3 and -0.8 , something that no longer occurred in subsequent outbursts. Excluding these first observational data, in the following outbursts during the maximum phase, the *B–V* color index assumed values between 0.09 and -0.05 , with an average value equal to $B-V=0.03$. Table 3 shows the mean values of the *B–V*, *V–R*, *R–I*, and *V–I* color indices calculated for AH Her in 2018, in phases of minimum and maximum brightness. Figure 15 shows a comparison between the light curve of AH Her in 2017 and the corresponding trend of the *B–V* color index.

As for the *V–R* color index, it varies between 0.01 and 0.19, with an average value of 0.12. Considering the limited data available, the mean value of $V-I_c$ is equal to 0.18 but this result is not significant. We also calculated the color indices of AH Her in the minimum light phase: *B–V* varies between 0.3 and 0.9, with an average value of 0.58, while *V–R* varies between 0.14

and 0.73, with an average value of 0.41—in excellent agreement with the value found by Spogli *et al.* (2001). As for the color indices estimated in 2018, they do not differ much from those calculated in 2017. At the minimum brightness of the star, the *B–V* varies between 0.22 and 0.69, while *V–R* varies between 0.22 and 0.67, *R–I* varies between 0.25 and 0.67, and *V–I* has values between 0.70 and 1.11.

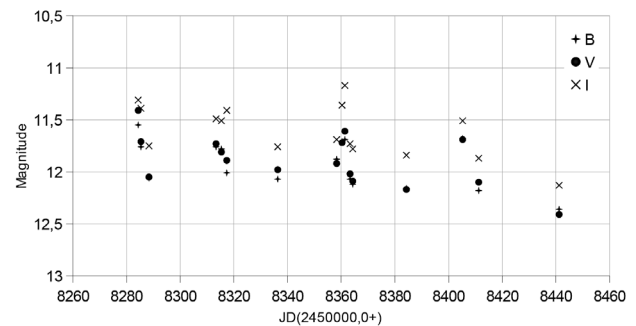


Figure 8. Representation of the maximum brightness values reached by AH Her in the various outbursts of 2018.

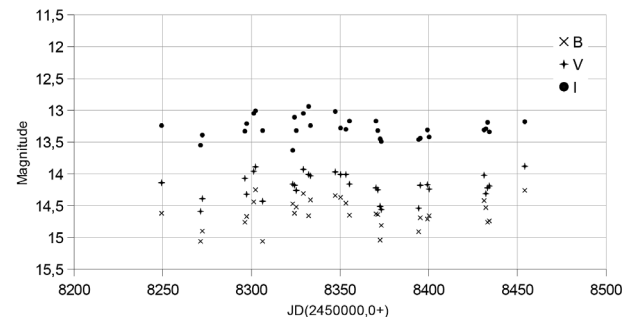


Figure 9. AH Her 2018 BVI_c light curve in the minimum light phase, constructed excluding the phases concerning the outbursts.

Clearly, the variable star has a variation of its spectral type when it reaches the maximum of the outburst from the phase of minimum light: AH Her tends to become bluer, and from type K it changes to type A, according to the Harvard classification; this is what can be deduced from the variation of the color indices.

During the various outbursts of the variable in 2018, in the maximum phase the B–V color index varies from –0.04 to 0.15, the V–R from –0.02 to 0.16, the R–I between 0.1 and 0.27, and the V–I between 0.1 and 0.48.

Figure 11 shows how the B–V color index varies as a function of the R_c magnitude: it can be seen that in the maximum phase the points accumulate around the value $B-V=0$ or are negative, while in the phase of minimum light the values of B–V are included between 0.3 and 1.

Figure 12 shows how the V– R_c color index varies as a function of the R_c magnitude in the year 2017: in the phase of maximum V– R_c has values between 0 and 0.2 while at minimum brightness V– R_c has values between 0.2 and 0.8.

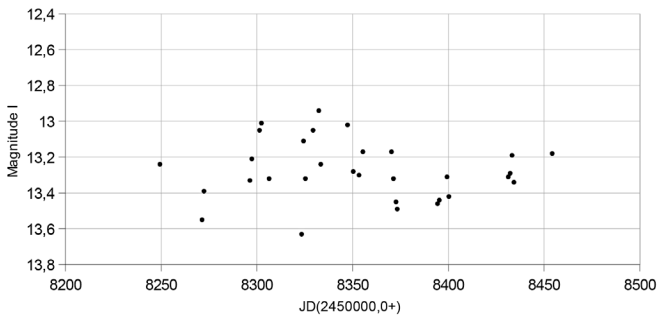


Figure 10. AH Her light curve in the minimum light phase, in the I_c band.

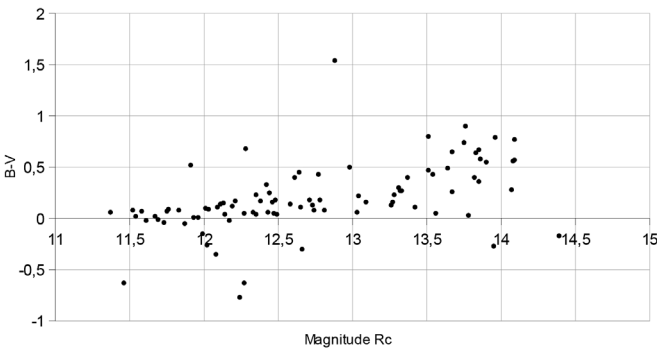


Figure 11. The B–V color index as a function of the magnitude R_c in 2017.

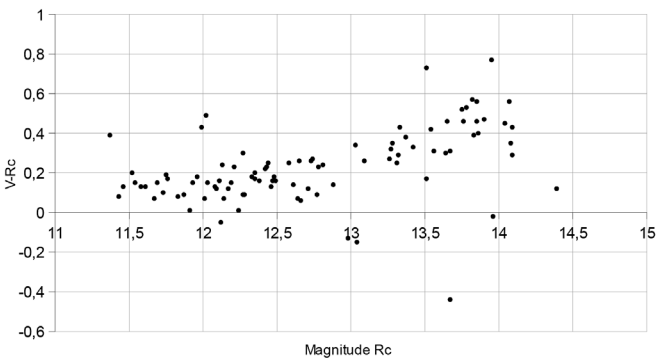


Figure 12. The V– R_c color index as a function of the magnitude R_c in 2017.

Figure 13 shows how the V– R_c color index varies as a function of time in the year 2017: we can see, comparing this graph with the light curve of AH Her, how V–R at the maximum brightness of the outbursts has values between 0 and 0.2, with some negative data, while in the minimum phase the values oscillate between 0.4 and 0.6, with peaks up to 0.8.

Figure 14 shows how the B–V color index varies as a function of time in the observations made in 2017: B–V is sharply negative in the rising phases preceding the outburst of the dwarf nova, assumes values between 0 and 0.1 at maximum, and values between 0.4 and 1.0 at minimum light.

Figure 15 shows a comparison between the AH Her light curve in 2017 and the corresponding change in the B–V color index. The color index assumes negative values during the maximum brightness of the outburst and positive values during the minimum brightness phase. During the standstill the B–V color index fluctuates around the value of zero.

In Figure 16 we can see how the V– I_c color index varies as a function of the V magnitude in the observations made in 2018. It may be noted that at the minimum the V– I_c values are between 0.6 and 1.2, while at the maximum V– I_c oscillates between 0.1 and 0.4. The overall trend of the points draws an arc of a parabola.

In Figure 17 we can see how the V– I_c color index varies as a function of time in the observations made in 2018. Clearly, during the numerous outbursts the V– I_c color index varies between 0.4 and 0.1, while in the phase of minimum light it oscillates between 0.7 and 1.1.

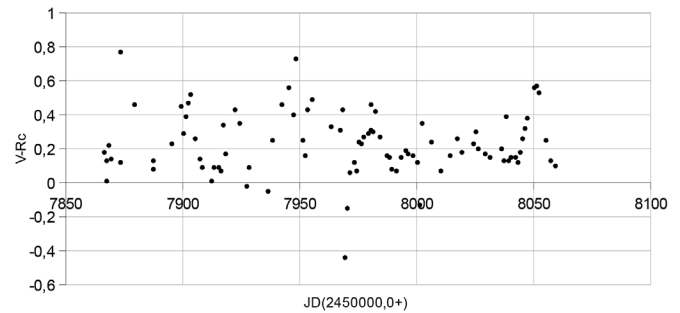


Figure 13. Variation of the V– R_c color index as a function of time in 2017.

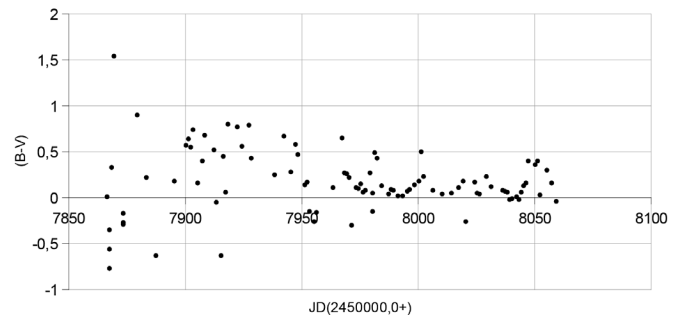


Figure 14. Variation of the B–V color index as a function of time in the observations made in 2017.

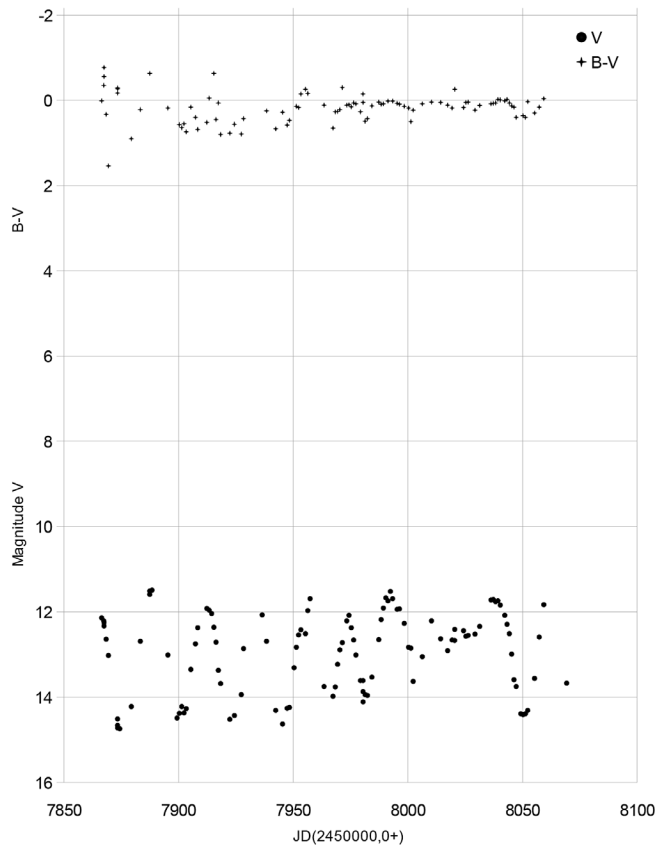


Figure 15. Variation of the B-V color index in relation to the trend of the light curve of AH Her in 2017.

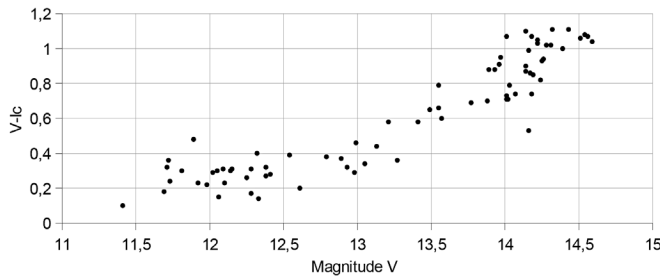


Figure 16. The $V-I_c$ color index as a function of the V magnitude in the 2018 observations.

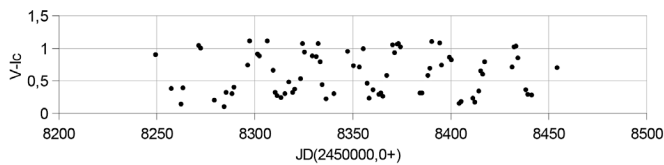


Figure 17. Variations of the $V-I_c$ color index with time in the 2018 observations.

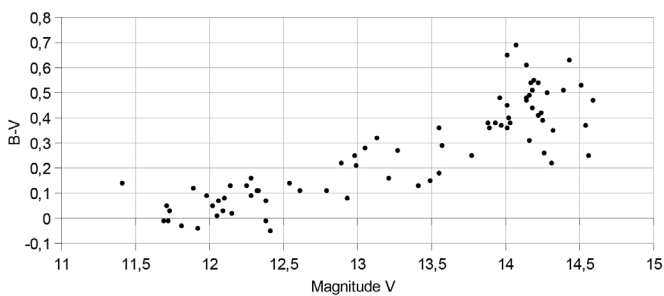


Figure 18. The B-V color index as a function of the V magnitude in the 2018 observations.

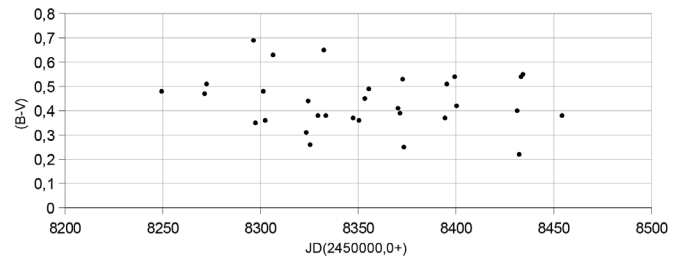


Figure 19. The B-V color index at a minimum in the 2018 observations: B-V values fluctuate between 0.2 and 0.7.

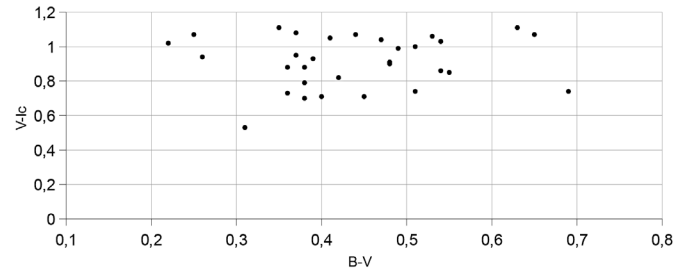


Figure 20. The color indices $V-I_c$ as a function of B-V at minimum light in the 2018 observations.

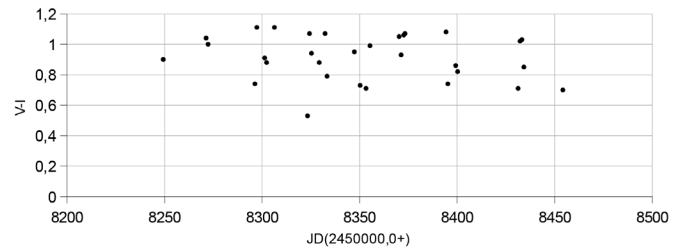


Figure 21. Distribution of the $V-I_c$ color index at a minimum as a function of time in 2018.

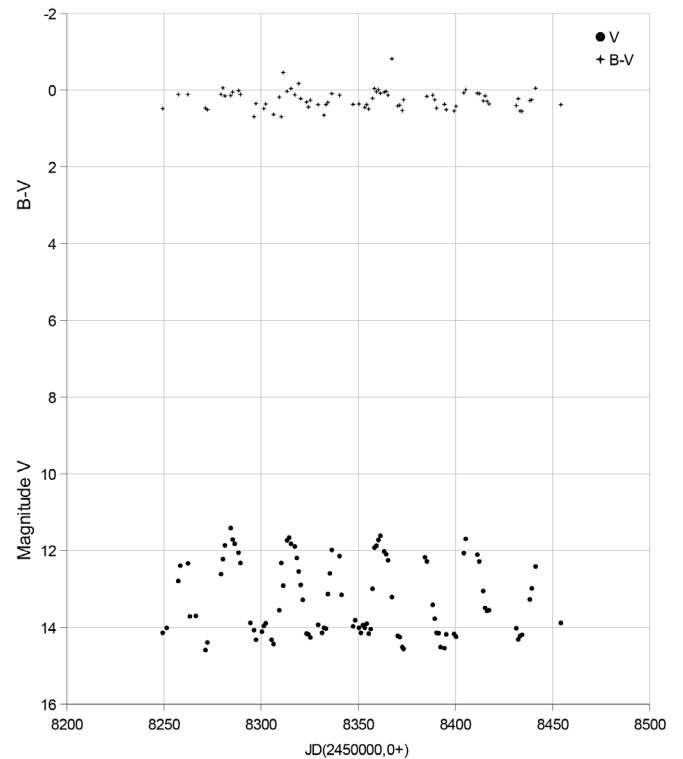


Figure 22. This figure shows the comparison between the light curve of AH Her in 2018 and the corresponding variation of the B-V color index referred to the same times and the same values of V magnitude.

In Figure 18 we can see how the color $B-V$ index varies as a function of the V magnitude for the observations made in 2018: in the minimum phase, $B-V$ is between 0.3 and 0.7, while at maximum, during the outburst $B-V$ varies between 0.2 and -0.1 . A negative $B-V$ color index indicates that the star emits more in the blue than in the visible.

Figures 19 and 21 show the variations of the $B-V$ and $V-I_c$ color indices in the phase of minimum light and as a function of time. These changes relate to AH Her observations made in 2018.

Figure 20 shows the distribution of the $V-I_c$ color index as a function of the $B-V$ color index in the minimum light phase for the observations relating to 2018; we have that $V-I_c$ is between 0.6 and 1.2, while $B-V$ oscillates between 0.2 and 0.7.

Figure 22 shows a comparison between the trend of the variation of the $B-V$ color index and the light curve of AH Her in 2018. We can note that in the phase of the maximum of the various outbursts, $B-V$ tends to assume negative values or close to zero, while in the phase of minimum light $B-V$ assumes positive values.

4. Typology of outbursts

The outbursts of dwarf novae have long been known to originate in the accretion disk surrounding the white dwarf (Smak 1971; Osaki 1974) due to a mechanism identified by Meyer and Meyer-Hofmeister (1981). This instability occurs when the temperature is low enough in the accretion disk that hydrogen recombines. The steep dependence of the opacity with temperature in this regime triggers a thermal and a viscous instability that leads the disk to cycle through two states. In the eruptive state, the disk has a high temperature $> 10,000$ K, hydrogen is highly ionized, and the mass accretion rate \dot{m}_M/\dot{m}_1 (M) from the disk on the white dwarf is higher than the mass transfer rate \dot{M}_1 from the companion star on the disk. In the quiescent state, the disk has a temperature < 3000 K, hydrogen is mostly neutral, and $\dot{M} < \dot{M}_1$. The disk instability model (DIM) aims at exploring the consequences of this instability on disk accretion and explaining the variety of observed light curves (Osaki 1996; Lasota 2001). Dwarf novae can have outbursts that are classified as type A or type B.

In type A outbursts, an outburst begins with the heating up and brightening of the outer parts of the disk; at the same time the viscosity increases, causing the material to flow inward and thus preventing an excessive heating of those outer parts. As the instability propagates, the inner parts become hotter and begin to contribute to the integrated luminosity. The type A outburst corresponds to higher levels of the mass-transfer rate. The outburst light curve has an asymmetrical profile. This asymmetric trend for AH Her can be seen in Figures 23 and 24; through linear regressions we have determined very different d_V/d_t between the phases of rise and the phases of decline.

In type B outbursts the instability occurs as a result of redistribution of the surface density in the inner parts of the disc and inward and outward propagation. Hence, the outburst begins almost simultaneously at all wavelengths and the emission is very strong in the U band. The instability of the B type outburst, starting in the inner parts of the disk and propagating outwards

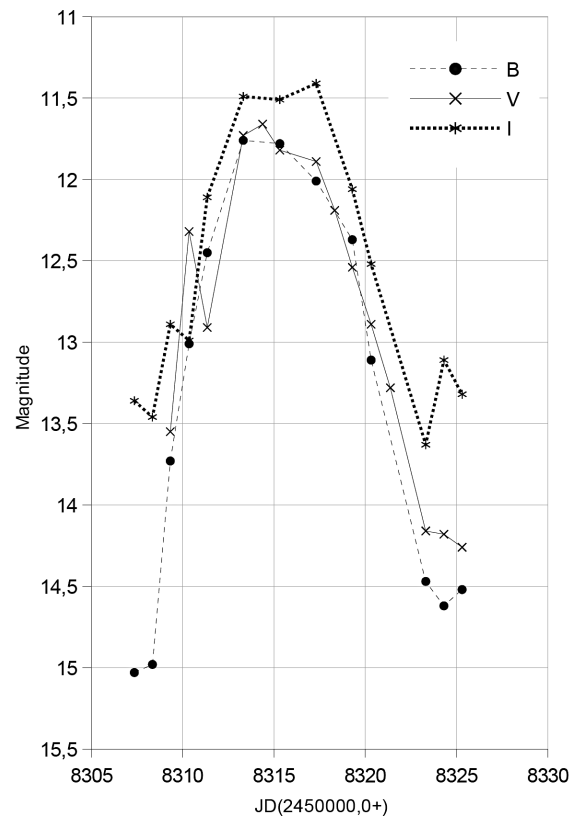


Figure 23. The outburst is slightly asymmetrical, since we have $d_V/d_t = -0.57$ mag/day in the ascent to the bright maximum, while $d_V/d_t = 0.38$ mag/day in the decline phase.

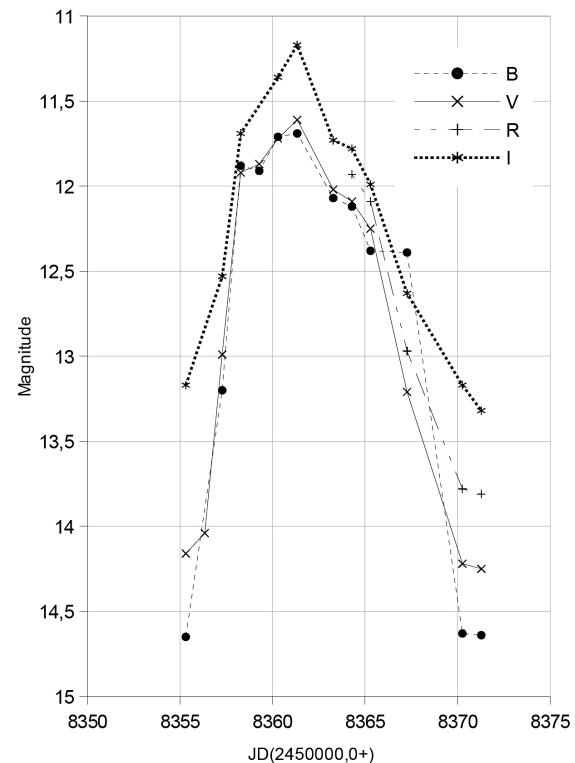


Figure 24. The outburst, which is a type A, is asymmetrical. The star rapidly increases in brightness and after reaching its maximum, it slowly declines. We have $d_V/d_t = -0.68$ mag/day for the maximum rise and $d_V/d_t = 0.30$ mag/day for the decline.

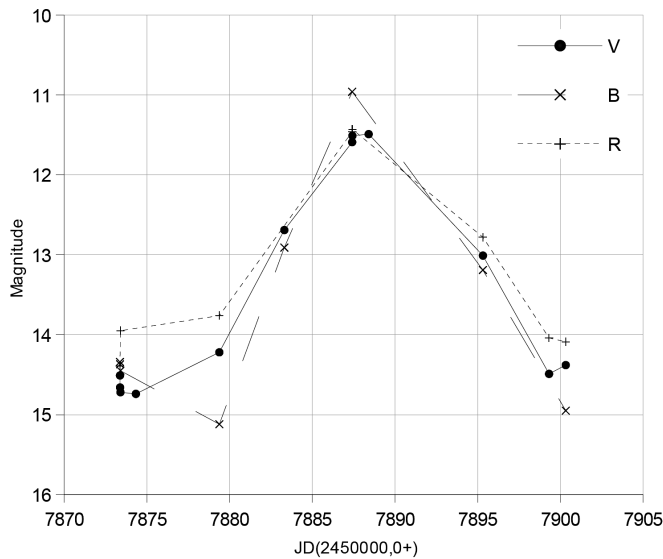


Figure 25. In this first example of a symmetrical outburst from 2017, the rise to maximum brightness expressed by $d_v/d_t = -0.31$ mag/day is almost equal to the decline time of $d_v/d_t = 0.25$ mag/day.

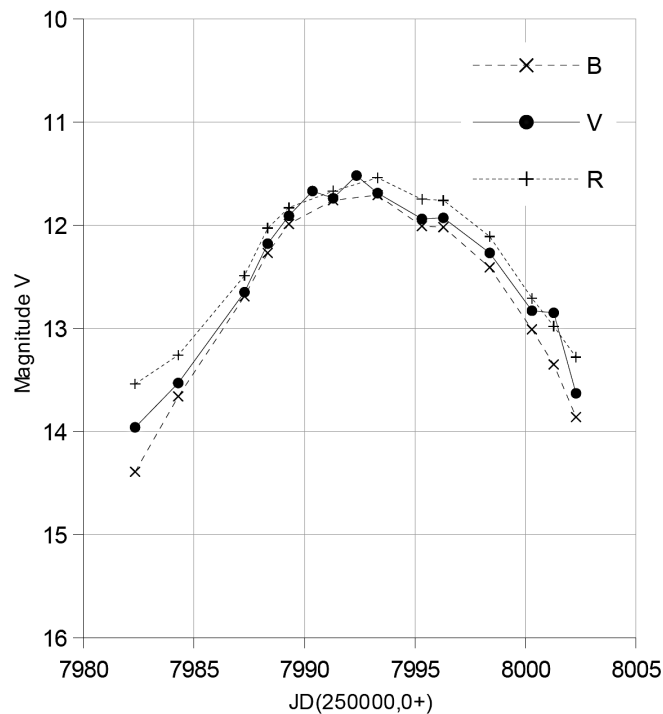


Figure 26. The outburst in this case is approximately symmetrical and the rise time at the maximum is almost equal to the decline time. We have $d_v/d_t = -0.23$ mag/day in the ascent phase and $d_v/d_t = 0.25$ mag/day in the decline.

(inside-out outburst), produces a rather symmetric light curve with a relatively low mass transfer rate (Smak 1984). In Figures 25, 26, and 27 we can see this type of outburst represented for AH Her; through linear regressions we have determined practically identical values of the d_v/d_t both for the phases of rise and for the phases of decline of the outbursts.

So as we can also see from the conformation of the light curves of the following outbursts, AH Her has both type A and type B outbursts.

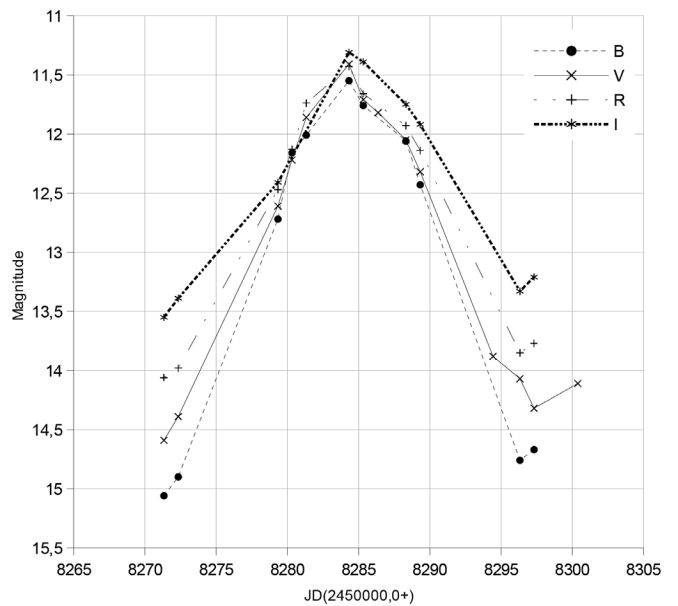


Figure 27. A typical Type B outburst: note that the light curve is almost symmetrical. The rate of climb at maximum light is equal to $d_v/d_t = -0.26$ mag/day, a value almost identical to that of decline which is $d_v/d_t = 0.24$ mag/day.

5. The intra-night time series in V band

We performed intra-night time series observations of AH Her on three nights: 05 May 2017, 27 September 2018, and 13 October 2018. The exposure time for each single observation was 240 seconds. Tables 4, 5, and 6 report the values of the estimated magnitudes for AH Her in the V band for these nights, while Table 7 reports the magnitudes of the star C8 (in the same field as AH Her) in the same bands.

In the observations of 05 May 2017 AH Her was in the phase of minimum light and the magnitude of the star varied by 0.5 magnitude, passing from $V = 14.2$ to $V = 14.7$. The star was tracked for about 1.9 hours in V, for a total of 15 photometric points. During this time the average value of AH Her was $V = 14.48 \pm 0.19$ magnitude, while the value of the reference star, C8 was $V(C8) = 12.58 \pm 0.02$ magnitude. Figures 28 and 29 show the trend of AH Her in the phase of minimum light.

In the observations of 27 September 2018, the star was in decline and the brightness of the variable went from $V = 13.7$ to $V = 14.0$, decreasing by 0.3 magnitude. In this phase AH Her was followed for 1.32 hours, 21 photometric points in the V band. The mean value of AH Her was $V = 13.89 \pm 0.09$ magnitude, while C8 had an average value equal to $V(C8) = 12.53 \pm 0.02$ magnitude. Figures 30 and 31 show the trend of AH Her in the phase of decline.

On 13 October 2018 AH her was followed in the maximum phase during an outburst for 0.93 hour. Its brightness did not vary, but remained constant around the mean value of $V = 11.7 \pm 0.03$ magnitude. A total of 14 photometric points were obtained. The average value of the star C8 in this third series of observations was $V(C8) = 12.51 \pm 0.03$ magnitude, a value which agrees with the previous data, but differs from the first data by 0.05 magnitude; this difference is within the margin of error. Figure 32 shows the trend of AH Her during the maximum brightness of this outburst.

Table 4. AH Her time series 5/05/2017.

| JD | V Magnitude | Error |
|-------------|-------------|-------|
| 2457879.379 | 14.22 | 0.01 |
| 2457879.401 | 14.19 | 0.01 |
| 2457879.406 | 14.29 | 0.03 |
| 2457879.408 | 14.24 | 0.03 |
| 2457879.412 | 14.22 | 0.02 |
| 2457879.423 | 14.43 | 0.02 |
| 2457879.427 | 14.61 | 0.04 |
| 2457879.431 | 14.51 | 0.03 |
| 2457879.435 | 14.56 | 0.02 |
| 2457879.437 | 14.63 | 0.02 |
| 2457879.441 | 14.59 | 0.01 |
| 2457879.447 | 14.68 | 0.02 |
| 2457879.451 | 14.65 | 0.02 |
| 2457879.454 | 14.71 | 0.02 |
| 2457879.458 | 14.69 | 0.02 |

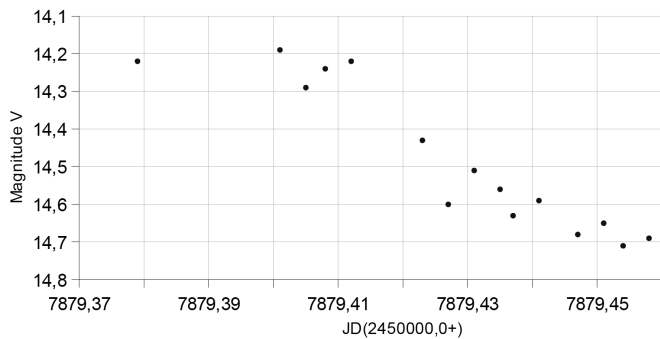


Figure 28. Time series in V from 05 May 2017. AH Her is in the phase of minimum light.

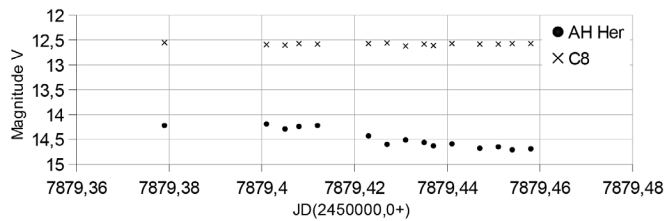


Figure 29. Time series in V from 05 May 2017 and comparison with the star C8 in the AH Her field.

6. Conclusions

We presented B, V, R_c , I_c observations of AH Her, a very active dwarf nova characterized by very frequent outbursts with recurrence times around 20 days. The variable star was systematically observed over the years 2017–2018 whenever the weather conditions allowed it. We can say that AH Her was particularly active and bright in 2017, reaching brightness values never reported before.

All observations were made at Gianni Rocchi's private observatory. The profile of the outbursts, which are both type A and type B, and the presence of a standstill even if of short duration in 2017 and of longer duration in 2012, confirm that this dwarf nova belongs to the Z Camelopardalis subgroup. Analyzing the 2017 AH Her standstill, we see that it does not end with a descent to the minimum as a classic Z Cam should do, but with a maximum rise of an outburst. This anomalous

Table 5. AH Her time series 27/09/2018.

| JD | V Magnitude | Error |
|-------------|-------------|-------|
| 2458389.281 | 13.77 | 0.03 |
| 2458389.283 | 13.86 | 0.01 |
| 2458389.286 | 13.82 | 0.02 |
| 2458389.289 | 13.76 | 0.01 |
| 2458389.291 | 13.77 | 0.01 |
| 2458389.294 | 13.73 | 0.03 |
| 2458389.297 | 13.82 | 0.03 |
| 2458389.301 | 13.84 | 0.02 |
| 2458389.303 | 13.87 | 0.02 |
| 2458389.305 | 13.90 | 0.04 |
| 2458389.308 | 13.82 | 0.01 |
| 2458389.311 | 13.92 | 0.03 |
| 2458389.314 | 13.92 | 0.01 |
| 2458389.317 | 13.92 | 0.04 |
| 2458389.319 | 13.97 | 0.05 |
| 2458389.322 | 13.94 | 0.01 |
| 2458389.325 | 13.98 | 0.01 |
| 2458389.328 | 14.03 | 0.04 |
| 2458389.331 | 14.01 | 0.01 |
| 2458389.334 | 13.97 | 0.08 |
| 2458389.336 | 13.98 | 0.03 |

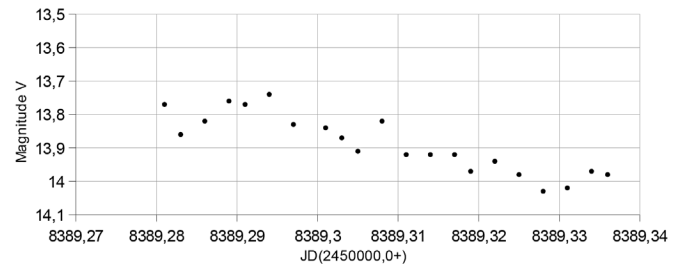


Figure 30. Time series in V from 27 September 2018. AH Her is in the decline phase.

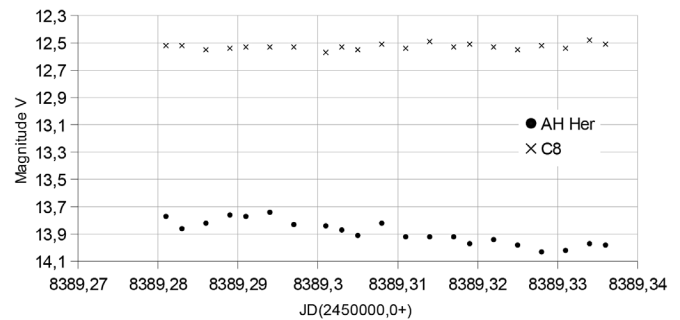


Figure 31. Time series in V from 27 September 2018 and comparison with the star C8 in the AH Her field.

behavior is typical of the IW And subclass of the Z Cams (Kato 2019). This unusual feature was identified for the first time by Wils *et al.* (2011).

The color indices are also typical of a dwarf nova of the Z Cam subgroup and correspond, in substantial agreement, with the color indices determined by other authors in the past years. The observations presented here are part of a project aimed to obtain light curves at different wavelengths of a certain sample of dwarf novae. This is being done in order to increase the information on and the historical database of this subgroup of cataclysmic variables, which can help astrophysicists in the construction of theoretical models closer to reality.

Table 6. AH Her time series 13/10/2018.

| JD | V Magnitude | Error |
|-------------|-------------|-------|
| 2458405.287 | 11.68 | 0.04 |
| 2458405.289 | 11.68 | 0.04 |
| 2458405.293 | 11.70 | 0.08 |
| 2458405.295 | 11.70 | 0.02 |
| 2458405.298 | 11.70 | 0.02 |
| 2458405.301 | 11.68 | 0.05 |
| 2458405.303 | 11.70 | 0.02 |
| 2458405.307 | 11.73 | 0.02 |
| 2458405.311 | 11.64 | 0.03 |
| 2458405.313 | 11.73 | 0.04 |
| 2458405.315 | 11.70 | 0.02 |
| 2458405.318 | 11.73 | 0.02 |
| 2458405.321 | 11.69 | 0.05 |
| 2458405.323 | 11.72 | 0.07 |

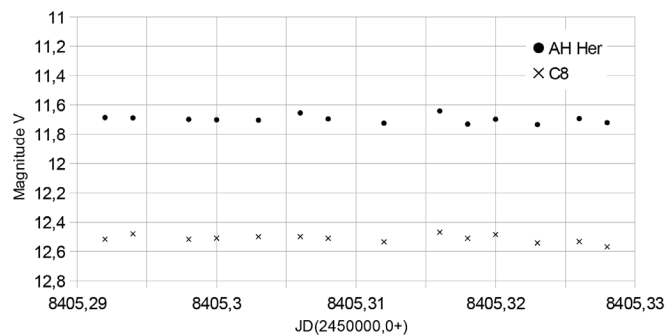


Figure 32. Time series in V from 13 October 2018 during the maximum of an AH Her outburst.

7. Acknowledgements

Special thanks to professor Rosella Piccotti who oversaw the English translation of our paper and warm thanks to the former Dean of the IIS Cassata Gattapone Professor Cecilia Tabarrini and her secretary Giancarlo Cerafischi, to the current Dean David Nadery, and to the Dean of the Liceo G. Mazzatinti of Gubbio, Maria Marinangeli for organizing seminars and conferences in their schools on themes of Astrophysics.

The most sincere thanks from professor Spogli Corrado to the direction of the Don Nicola Mazza College of Padua for having helped him financially during the period of time in which he attended the faculty of Astromomy at the University of Padua where he then graduated.

References

Bruch, A. 1984, *Astron. Astrophys., Suppl. Ser.*, **56**, 441.
 Chevalier, C., and Ilovaisky, S. A. 1991, *Astron. Astrophys., Suppl. Ser.*, **90**, 225.
 Echevarria, J., et al. 2021, *Mon. Not. Roy. Astron. Soc.*, **501**, 596.
 Hellier, C. 2001, *Cataclysmic Variable Stars*, Springer, New York.
 Horne, K., Wade, R. A., and Szkody, P. 1986, *Mon. Not. Roy. Astron. Soc.*, **219**, 791.
 Kato, T. 2015, *Publ. Astron. Soc. Japan*, **67**, 108.
 Kato, T. 2019, *Publ. Astron. Soc. Japan*, **71**, 20.

Table 7. Time series observations of the star C8.

| JD | V (C8) | Error | JD | V (C8) | Error |
|-------------|--------|-------|-------------|--------|-------|
| 2457879.379 | 12.55 | 0.12 | 2458389.308 | 12.50 | 0.04 |
| 2457879.401 | 12.59 | 0.01 | 2458389.311 | 12.54 | 0.01 |
| 2457879.406 | 12.60 | 0.02 | 2458389.314 | 12.50 | 0.03 |
| 2457879.408 | 12.57 | 0.02 | 2458389.317 | 12.54 | 0.01 |
| 2457879.412 | 12.58 | 0.03 | 2458389.319 | 12.49 | 0.04 |
| 2457879.423 | 12.57 | 0.01 | 2458389.322 | 12.53 | 0.05 |
| 2457879.427 | 12.56 | 0.02 | 2458389.325 | 12.55 | 0.01 |
| 2457879.431 | 12.62 | 0.03 | 2458389.328 | 12.51 | 0.03 |
| 2457879.435 | 12.58 | 0.01 | 2458389.331 | 12.53 | 0.01 |
| 2457879.437 | 12.61 | 0.01 | 2458389.334 | 12.48 | 0.09 |
| 2457879.441 | 12.57 | 0.02 | 2458389.336 | 12.50 | 0.03 |
| 2457879.447 | 12.58 | 0.01 | 2458405.287 | 12.52 | 0.05 |
| 2457879.451 | 12.58 | 0.02 | 2458405.289 | 12.48 | 0.04 |
| 2457879.454 | 12.57 | 0.02 | 2458405.293 | 12.52 | 0.08 |
| 2457879.458 | 12.57 | 0.01 | 2458405.295 | 12.51 | 0.02 |
| 2458389.281 | 12.52 | 0.02 | 2458405.298 | 12.50 | 0.02 |
| 2458389.283 | 12.52 | 0.01 | 2458405.301 | 12.50 | 0.05 |
| 2458389.286 | 12.55 | 0.02 | 2458405.303 | 12.51 | 0.02 |
| 2458389.289 | 12.54 | 0.01 | 2458405.307 | 12.53 | 0.01 |
| 2458389.291 | 12.53 | 0.01 | 2458405.311 | 12.47 | 0.03 |
| 2458389.294 | 12.53 | 0.02 | 2458405.313 | 12.51 | 0.05 |
| 2458389.297 | 12.53 | 0.02 | 2458405.315 | 12.48 | 0.01 |
| 2458389.301 | 12.57 | 0.02 | 2458405.318 | 12.54 | 0.02 |
| 2458389.303 | 12.53 | 0.02 | 2458405.321 | 12.53 | 0.05 |
| 2458389.305 | 12.55 | 0.03 | 2458405.323 | 12.57 | 0.05 |

Note: C8 coordinates (2000.0) = R.A. 16^h 43^m 52^s Dec. +25° 11' 34".

Kato, T., Nogami, D., Baba, H., Masuda, S., Matsumoto, K., and Kunjaya, C. 1999, in *Disk Instabilities in Close Binary Systems. 25 Years of the Disk-Instability Model*, eds. S. Mineshige, J. C. Wheeler, Frontiers Sci. Ser. 26, Universal Academy Press, Inc., Tokyo, 45.
 Lasota, J.-P. 2001, *New Astron. Rev.*, **45**, 449.
 Meyer, F., and Meyer-Hofmeister, E. 1981, *Astron. Astrophys.*, **104**, L10.
 Misselt, K. A. 1996, *Publ. Astron. Soc. Pacific*, **108**, 146.
 Osaki, Y. 1974, *Publ. Astron. Soc. Japan*, **26**, 429.
 Osaki, Y. 1996, *Publ. Astron. Soc. Pacific*, **108**, 39.
 Ramsay G., Scheiber M., Gensicke B. T., and Wheatley, P. J. 2017, *Astron. Astrophys.*, **604A**, 107.
 Ritter, H., and Kolb U. 1998, *Astron. Astrophys., Suppl. Ser.*, **129**, 83.
 Smak, J. 1971, *Acta Astron.*, **21**, 15.
 Smak, J. 1983, *Astrophys. J.*, **272**, 234.
 Smak, J. 1984, *Acta Astron.*, **34**, 161.
 Spogli, C., Fiorucci, M., Tosti, G., and Raimondo, G. 2001, *Inf. Bull. Var. Stars*, No. 5147, 1.
 Verbunt, F., Bunk, W. H., Ritter, H., and Pfeffermann E. 1997, *Astron. Astrophys.*, **327**, 602.
 Verbunt, F., et al. 1984, *Mon. Not. Roy. Astron. Soc.*, **210**, 197.
 Warner, B. 1995, *Cataclysmic Variable Stars*, Cambridge Univ. Press, Cambridge.
 Warner, B. 2003, *Cataclysmic Variable Stars*, Cambridge Univ. Press, Cambridge (doi:10.1017/CB09780511586491).
 Williams, G. 1983, *Astrophys. J., Suppl. Ser.*, **53**, 523.
 Wils, P., Gänsicke, B. T., Drake, A. J., and Southworth, J. 2010, *Mon. Not. Roy. Astron. Soc.*, **402**, 436.
 Wils, P., Krajci, T., and Simonsen, M. 2011, *J. Amer. Assoc. Var. Star Obs.*, **39**, 77.

Appendix A: B, V, R_c, I_c observed magnitude data for the dwarf nova AH Her during the years 2012, 2014, 2017, and 2018.

| <i>Date</i> | <i>JD(2450000.0+)</i> | <i>B</i> | <i>Error</i> | <i>V</i> | <i>Error</i> | <i>R_c</i> | <i>Error</i> | <i>I_c</i> | <i>Error</i> |
|-------------------|-----------------------|----------|--------------|----------|--------------|----------------------|--------------|----------------------|--------------|
| 10 July 2012 | 6120.33 | — | — | 12.49 | 0.05 | — | — | — | — |
| 12 July 2012 | 6121.33 | — | — | 12.53 | 0.02 | — | — | — | — |
| 16 July 2012 | 6125.38 | — | — | 12.52 | 0.03 | — | — | — | — |
| 18 July 2012 | 6127.47 | — | — | 12.58 | 0.03 | — | — | — | — |
| 19 July 2012 | 6128.34 | — | — | 12.59 | 0.03 | — | — | — | — |
| 26 July 2012 | 6135.34 | — | — | 12.58 | 0.03 | — | — | — | — |
| 29 July 2012 | 6138.32 | — | — | 12.56 | 0.02 | — | — | — | — |
| 30 July 2012 | 6139.32 | — | — | 12.55 | 0.02 | — | — | — | — |
| 31 July 2012 | 6140.32 | — | — | 12.60 | 0.02 | — | — | — | — |
| 01 August 2012 | 6141.35 | — | — | 12.61 | 0.02 | — | — | — | — |
| 02 August 2012 | 6142.33 | — | — | 12.63 | 0.02 | — | — | — | — |
| 05 August 2012 | 6145.32 | — | — | 12.57 | 0.04 | — | — | — | — |
| 06 August 2012 | 6146.31 | — | — | 12.61 | 0.03 | — | — | — | — |
| 07 August 2012 | 6147.23 | — | — | 12.66 | 0.03 | — | — | — | — |
| 08 August 2012 | 6148.32 | — | — | 12.69 | 0.02 | — | — | — | — |
| 09 August 2012 | 6149.31 | — | — | 12.61 | 0.01 | — | — | — | — |
| 10 August 2012 | 6150.32 | — | — | 12.88 | 0.04 | — | — | — | — |
| 19 August 2012 | 6159.40 | — | — | — | — | 12.72 | 0.02 | — | — |
| 20 August 2012 | 6160.30 | — | — | 12.86 | 0.02 | — | — | — | — |
| 21 August 2012 | 6161.33 | — | — | — | — | 12.69 | 0.07 | — | — |
| 22 August 2012 | 6162.32 | — | — | 12.74 | 0.03 | — | — | — | — |
| 23 August 2012 | 6163.30 | — | — | 12.71 | 0.02 | — | — | — | — |
| 24 August 2012 | 6164.30 | — | — | — | — | 12.61 | 0.05 | — | — |
| 25 August 2012 | 6165.34 | — | — | — | — | 12.59 | 0.02 | — | — |
| 03 September 2012 | 6174.33 | — | — | 12.54 | 0.03 | — | — | — | — |
| 06 September 2012 | 6177.28 | — | — | 12.65 | 0.01 | — | — | — | — |
| 07 September 2012 | 6178.28 | — | — | — | — | 12.51 | 0.02 | — | — |
| 08 September 2012 | 6179.31 | — | — | — | — | 12.46 | 0.02 | — | — |
| 10 September 2012 | 6181.27 | — | — | 12.67 | 0.06 | — | — | — | — |
| 11 September 2012 | 6182.27 | — | — | 12.63 | 0.01 | — | — | — | — |
| 15 September 2012 | 6186.32 | — | — | — | — | 12.35 | 0.03 | — | — |
| 16 September 2012 | 6187.27 | — | — | 12.53 | 0.04 | — | — | — | — |
| 17 September 2012 | 6188.27 | — | — | 12.61 | 0.02 | — | — | — | — |
| 21 September 2012 | 6192.33 | — | — | 12.53 | 0.03 | — | — | — | — |
| 22 September 2012 | 6193.27 | — | — | 12.49 | 0.03 | — | — | — | — |
| 03 October 2012 | 6204.24 | — | — | 12.31 | 0.02 | — | — | — | — |
| 05 October 2012 | 6206.24 | — | — | 12.26 | 0.02 | — | — | — | — |
| 06 October 2012 | 6207.23 | — | — | 12.34 | 0.04 | — | — | — | — |
| 17 October 2012 | 6218.26 | — | — | 12.62 | 0.04 | — | — | — | — |
| 18 October 2012 | 6219.24 | — | — | 12.57 | 0.02 | — | — | — | — |
| 19 October 2012 | 6220.23 | — | — | 12.66 | 0.02 | — | — | — | — |
| 20 October 2012 | 6221.24 | — | — | 12.69 | 0.02 | — | — | — | — |
| 22 October 2012 | 6223.23 | — | — | 12.74 | 0.05 | — | — | — | — |
| 23 October 2012 | 6224.27 | — | — | 12.69 | 0.01 | — | — | — | — |
| 24 October 2012 | 6225.25 | — | — | 12.55 | 0.05 | — | — | — | — |
| 25 October 2012 | 6226.22 | — | — | 12.47 | 0.03 | — | — | — | — |
| 29 October 2012 | 6230.28 | — | — | 12.71 | 0.02 | — | — | — | — |
| 01 November 2012 | 6233.21 | — | — | 12.53 | 0.05 | — | — | — | — |
| 07 November 2012 | 6239.21 | — | — | 12.62 | 0.02 | — | — | — | — |
| 03 August 2014 | 6873.36 | — | — | 14.11 | 0.04 | 13.69 | 0.04 | — | — |
| 11 August 2014 | 6881.31 | — | — | 12.14 | 0.04 | 12.04 | 0.01 | — | — |
| 12 August 2014 | 6882.32 | — | — | — | — | 12.26 | 0.02 | 12.21 | 0.01 |
| 16 August 2014 | 6886.40 | — | — | 14.09 | 0.03 | — | — | — | — |
| 24 August 2014 | 6894.30 | — | — | — | — | 12.01 | 0.02 | — | — |
| 29 August 2014 | 6899.31 | — | — | 13.09 | 0.02 | — | — | 12.57 | 0.04 |
| 06 September 2014 | 6907.29 | — | — | 13.59 | 0.03 | — | — | 12.91 | 0.01 |
| 14 September 2014 | 6915.28 | 11.73 | 0.02 | 11.75 | 0.02 | — | — | — | — |
| 22 September 2014 | 6923.28 | 14.57 | 0.08 | 14.01 | 0.02 | — | — | — | — |
| 26 September 2014 | 6927.30 | — | — | 13.92 | 0.01 | — | — | 13.14 | 0.03 |
| 27 September 2014 | 6928.31 | — | — | — | — | — | — | 12.99 | 0.01 |
| 29 September 2014 | 6930.30 | — | — | 12.17 | 0.02 | — | — | 11.88 | 0.05 |
| 04 October 2014 | 6935.33 | — | — | 13.99 | 0.02 | — | — | 13.21 | 0.05 |
| 08 October 2014 | 6939.27 | 14.38 | 0.06 | 13.93 | 0.02 | 13.41 | 0.02 | — | — |
| 09 October 2014 | 6940.25 | 14.19 | 0.02 | 13.59 | 0.01 | — | — | — | — |
| 11 October 2014 | 6942.31 | — | — | 12.32 | 0.03 | — | — | 11.84 | 0.05 |
| 18 October 2014 | 6949.27 | — | — | 14.03 | 0.05 | — | — | 13.15 | 0.05 |
| 22 October 2014 | 6953.24 | — | — | 13.49 | 0.03 | 12.96 | 0.01 | — | — |

Table continued on following pages

Appendix A: B, V, R_c, I_c observed magnitude data for the dwarf nova AH Her during the years 2012, 2014, 2017, and 2018 (cont).

| <i>Date</i> | <i>JD(2450000.0+)</i> | <i>B</i> | <i>Error</i> | <i>V</i> | <i>Error</i> | <i>R_c</i> | <i>Error</i> | <i>I_c</i> | <i>Error</i> |
|-----------------|-----------------------|----------|--------------|----------|--------------|----------------------|--------------|----------------------|--------------|
| 25 October 2014 | 6956.24 | — | — | 12.26 | 0.04 | 12.11 | 0.03 | — | — |
| 27 October 2014 | 6958.27 | — | — | 12.74 | 0.01 | 12.52 | 0.02 | — | — |
| 29 October 2014 | 6959.21 | 13.53 | 0.03 | 13.18 | 0.03 | 12.94 | 0.02 | — | — |
| 22 April 2017 | 7866.44 | 12.15 | 0.05 | 12.14 | 0.02 | 11.96 | 0.05 | — | — |
| 23 April 2017 | 7867.46 | 11.86 | 0.07 | 12.21 | 0.04 | 12.08 | 0.02 | — | — |
| 23 April 2017 | 7867.47 | 11.48 | 0.05 | 12.25 | 0.03 | — | — | — | — |
| 23 April 2017 | 7867.47 | 11.77 | 0.08 | 12.33 | 0.04 | 12.24 | 0.02 | 12.11 | 0.03 |
| 24 April 2017 | 7868.40 | 12.87 | 0.05 | 12.64 | 0.06 | 12.42 | 0.05 | — | — |
| 25 April 2017 | 7869.39 | 14.56 | 0.03 | 13.02 | 0.08 | 12.88 | 0.05 | — | — |
| 29 April 2017 | 7873.37 | 14.34 | 0.04 | 14.51 | 0.07 | — | — | — | — |
| 29 April 2017 | 7973.38 | 14.37 | 0.05 | 14.66 | 0.03 | 14.39 | 0.05 | 13.88 | 0.04 |
| 29 April 2017 | 7973.40 | 14.45 | 0.03 | 14.72 | 0.04 | 13.95 | 0.05 | 13.40 | 0.06 |
| 30 April 2017 | 7874.33 | — | — | 14.74 | 0.04 | — | — | — | — |
| 05 May 2017 | 7879.38 | 15.12 | 0.05 | 14.22 | 0.02 | 13.76 | 0.02 | 13.21 | 0.05 |
| 09 May 2017 | 7883.31 | 12.91 | 0.05 | 12.69 | 0.07 | — | — | — | — |
| 13 May 2017 | 7887.41 | 10.96 | 0.04 | 11.59 | 0.05 | 11.46 | 0.04 | 11.38 | 0.05 |
| 13 May 2017 | 7887.41 | — | — | 11.43 | 0.02 | 11.43 | 0.02 | — | — |
| 14 May 2017 | 7888.41 | — | — | 11.49 | 0.07 | — | — | — | — |
| 21 May 2017 | 7895.32 | 13.19 | 0.05 | 13.01 | 0.08 | 12.78 | 0.03 | — | — |
| 25 May 2017 | 7899.31 | — | — | 14.49 | 0.07 | 14.04 | 0.02 | — | — |
| 26 May 2017 | 7900.32 | 14.95 | 0.02 | 14.38 | 0.05 | 14.09 | 0.04 | 13.24 | 0.02 |
| 27 May 2017 | 7901.36 | 14.86 | 0.11 | 14.22 | 0.02 | 13.83 | 0.02 | — | — |
| 28 May 2017 | 7902.33 | 14.92 | 0.09 | 14.37 | 0.02 | 13.90 | 0.05 | — | — |
| 29 May 2017 | 7903.33 | 15.01 | 0.03 | 14.27 | 0.02 | 13.75 | 0.03 | — | — |
| 31 May 2017 | 7905.32 | 13.51 | 0.05 | 13.35 | 0.02 | 13.09 | 0.05 | — | — |
| 02 June 2017 | 7907.35 | 13.15 | 0.05 | 12.75 | 0.02 | 12.61 | 0.03 | — | — |
| 03 June 2017 | 7908.33 | 13.05 | 0.01 | 12.37 | 0.04 | 12.28 | 0.04 | — | — |
| 07 June 2017 | 7912.32 | 12.44 | 0.03 | 11.92 | 0.05 | 11.91 | 0.08 | — | — |
| 08 June 2017 | 7913.33 | 11.91 | 0.08 | 11.96 | 0.02 | 11.87 | 0.02 | — | — |
| 09 June 2017 | 7914.41 | — | — | 12.03 | 0.03 | — | — | — | — |
| 10 June 2017 | 7915.38 | 11.73 | 0.05 | 12.36 | 0.03 | 12.27 | 0.04 | 12.13 | 0.02 |
| 11 June 2017 | 7916.32 | 13.16 | 0.15 | 12.71 | 0.16 | 12.64 | 0.04 | — | — |
| 12 June 2017 | 7917.32 | 14.43 | 0.18 | 13.37 | 0.06 | 13.03 | 0.07 | — | — |
| 13 June 2017 | 7918.32 | 14.48 | 0.05 | 13.68 | 0.16 | 13.51 | 0.07 | — | — |
| 17 June 2017 | 7922.33 | 15.29 | 0.12 | 14.52 | 0.07 | 14.09 | 0.02 | — | — |
| 19 June 2017 | 7924.33 | 14.99 | 0.02 | 14.43 | 0.02 | 14.08 | 0.05 | — | — |
| 22 June 2017 | 7927.33 | 14.73 | 0.21 | 13.94 | 0.09 | 13.96 | 0.03 | — | — |
| 23 June 2017 | 7928.32 | 13.29 | 0.09 | 13.27 | 0.17 | 12.77 | 0.02 | — | — |
| 01 July 2017 | 7936.44 | — | — | 12.07 | 0.03 | 12.12 | 0.04 | 11.78 | 0.03 |
| 04 July 2017 | 7938.34 | 12.94 | 0.09 | 12.69 | 0.02 | 12.44 | 0.05 | — | — |
| 07 July 2017 | 7942.34 | 14.98 | 0.11 | 14.31 | 0.02 | 13.85 | 0.04 | — | — |
| 10 July 2017 | 7945.32 | 14.91 | 0.03 | 14.63 | 0.01 | 14.07 | 0.04 | — | — |
| 12 July 2017 | 7947.33 | 14.84 | 0.09 | 14.26 | 0.06 | 13.86 | 0.03 | — | — |
| 13 July 2017 | 7948.33 | 14.71 | 0.08 | 14.24 | 0.02 | 13.51 | 0.07 | — | — |
| 15 July 2017 | 7950.35 | — | — | 13.31 | 0.03 | — | — | — | — |
| 16 July 2017 | 7951.33 | 12.97 | 0.06 | 12.83 | 0.04 | 12.58 | 0.08 | — | — |
| 17 July 2017 | 7952.32 | 12.71 | 0.05 | 12.54 | 0.05 | 12.38 | 0.05 | — | — |
| 18 July 2017 | 7953.32 | 12.27 | 0.06 | 12.42 | 0.02 | 11.99 | 0.08 | — | — |
| 20 July 2017 | 7955.32 | 12.25 | 0.05 | 12.51 | 0.02 | 12.02 | 0.05 | — | — |
| 21 July 2017 | 7956.32 | 11.81 | 0.05 | 11.97 | 0.05 | — | — | — | — |
| 22 July 2017 | 7957.34 | — | — | 11.69 | 0.04 | — | — | — | — |
| 28 July 2017 | 7963.41 | 13.86 | 0.05 | 13.75 | 0.04 | 13.42 | 0.06 | — | — |
| 01 August 2017 | 7967.31 | 14.63 | 0.05 | 13.98 | 0.06 | 13.67 | 0.05 | — | — |
| 02 August 2017 | 7968.32 | 14.03 | 0.02 | 13.76 | 0.06 | 13.33 | 0.03 | — | — |
| 03 August 2017 | 7969.32 | 13.49 | 0.06 | 13.23 | 0.07 | 13.67 | 0.05 | — | — |
| 04 August 2017 | 7970.33 | 13.11 | 0.08 | 12.89 | 0.02 | 13.04 | 0.09 | — | — |
| 05 August 2017 | 7971.40 | 12.42 | 0.05 | 12.72 | 0.04 | 12.66 | 0.05 | 12.63 | 0.04 |
| 07 August 2017 | 7973.33 | 12.32 | 0.03 | 12.21 | 0.03 | 12.09 | 0.02 | — | — |
| 08 August 2017 | 7974.31 | 12.18 | 0.03 | 12.08 | 0.05 | 12.01 | 0.02 | — | — |
| 09 August 2017 | 7975.30 | 12.52 | 0.12 | 12.37 | 0.02 | 12.13 | 0.03 | — | — |
| 10 August 2017 | 7976.33 | 12.72 | 0.02 | 12.66 | 0.02 | 12.43 | 0.01 | — | — |
| 11 August 2017 | 7977.31 | 13.09 | 0.05 | 13.01 | 0.01 | 12.74 | 0.01 | — | — |
| 13 August 2017 | 7979.31 | 13.88 | 0.06 | 13.61 | 0.02 | 13.32 | 0.07 | — | — |
| 14 August 2017 | 7980.40 | 13.46 | 0.08 | 13.64 | 0.04 | — | — | 13.18 | 0.03 |
| 14 August 2017 | 7980.42 | 13.92 | 0.09 | 13.87 | 0.02 | 13.66 | 0.04 | 13.09 | 0.05 |
| 14 August 2017 | 7980.44 | — | — | 14.11 | 0.03 | — | — | — | — |
| 15 August 2017 | 7981.3 | 14.43 | 0.03 | 13.94 | 0.02 | 13.62 | 0.05 | — | — |
| 16 August 2017 | 7982.33 | 14.39 | 0.03 | 13.96 | 0.02 | 13.54 | 0.11 | — | — |

Table continued on following pages

Appendix A: B, V, R_c, I_c observed magnitude data for the dwarf nova AH Her during the years 2012, 2014, 2017, and 2018 (cont).

| <i>Date</i> | <i>JD(2450000.0+)</i> | <i>B</i> | <i>Error</i> | <i>V</i> | <i>Error</i> | <i>R_c</i> | <i>Error</i> | <i>I_c</i> | <i>Error</i> |
|-------------------|-----------------------|----------|--------------|----------|--------------|----------------------|--------------|----------------------|--------------|
| 18 August 2017 | 7984.29 | 13.66 | 0.03 | 13.53 | 0.04 | 13.28 | 0.13 | — | — |
| 21 August 2017 | 7987.29 | 12.69 | 0.02 | 12.65 | 0.02 | 12.49 | 0.07 | — | — |
| 22 August 2017 | 7988.33 | 12.27 | 0.05 | 12.18 | 0.03 | 12.03 | 0.03 | — | — |
| 23 August 2017 | 7989.29 | 11.99 | 0.08 | 11.91 | 0.02 | 11.83 | 0.04 | — | — |
| 24 August 2017 | 7990.36 | — | — | 11.67 | 0.05 | — | — | — | — |
| 25 August 2017 | 7991.30 | 11.76 | 0.02 | 11.74 | 0.02 | 11.67 | 0.02 | — | — |
| 26 August 2017 | 7992.35 | — | — | 11.52 | 0.02 | — | — | 11.38 | 0.03 |
| 27 August 2017 | 7993.31 | 11.71 | 0.03 | 11.69 | 0.08 | 11.54 | 0.03 | — | — |
| 29 August 2017 | 7995.31 | 12.01 | 0.05 | 11.94 | 0.04 | 11.75 | 0.04 | — | — |
| 30 August 2017 | 7996.28 | 12.02 | 0.04 | 11.93 | 0.04 | 11.76 | 0.02 | — | — |
| 01 September 2017 | 7998.38 | 12.41 | 0.03 | 12.27 | 0.03 | 12.11 | 0.02 | — | — |
| 03 September 2017 | 8000.29 | 13.01 | 0.08 | 12.83 | 0.08 | 12.71 | 0.04 | — | — |
| 04 September 2017 | 8001.27 | 13.35 | 0.07 | 12.85 | 0.07 | 12.98 | 0.05 | — | — |
| 05 September 2017 | 8002.28 | 13.86 | 0.08 | 13.63 | 0.08 | 13.28 | 0.02 | — | — |
| 09 September 2017 | 8006.27 | 13.13 | 0.03 | 13.06 | 0.03 | 12.81 | 0.02 | — | — |
| 13 September 2017 | 8010.27 | 12.25 | 0.02 | 12.21 | 0.02 | 12.14 | 0.03 | — | — |
| 17 September 2017 | 8014.25 | 12.68 | 0.03 | 12.63 | 0.03 | 12.47 | 0.03 | — | — |
| 20 September 2017 | 8017.32 | 13.02 | 0.02 | 12.91 | 0.02 | 12.65 | 0.05 | — | — |
| 22 September 2017 | 8018.27 | 12.84 | 0.04 | 12.66 | 0.04 | 12.48 | 0.02 | — | — |
| 23 September 2017 | 8020.36 | — | — | 12.67 | 0.06 | — | — | 12.13 | 0.05 |
| 23 September 2017 | 8020.40 | 12.15 | 0.05 | 12.41 | 0.05 | — | — | 12.15 | 0.04 |
| 27 September 2017 | 8024.25 | 12.61 | 0.02 | 12.44 | 0.05 | 12.21 | 0.08 | — | — |
| 28 September 2017 | 8025.26 | 12.62 | 0.02 | 12.57 | 0.02 | 12.27 | 0.09 | — | — |
| 29 September 2017 | 8026.26 | 12.59 | 0.04 | 12.55 | 0.02 | 12.36 | 0.04 | — | — |
| 02 October 2017 | 8029.25 | 12.75 | 0.07 | 12.52 | 0.02 | 12.35 | 0.03 | — | — |
| 04 October 2017 | 8031.29 | 12.46 | 0.05 | 12.34 | 0.02 | 12.19 | 0.03 | — | — |
| 09 October 2017 | 8036.29 | 11.80 | 0.05 | 11.72 | 0.02 | 11.52 | 0.02 | — | — |
| 10 October 2017 | 8037.24 | 11.78 | 0.03 | 11.71 | 0.02 | 11.58 | 0.03 | — | — |
| 11 October 2017 | 8038.22 | 11.82 | 0.05 | 11.76 | 0.05 | 11.37 | 0.03 | — | — |
| 12 October 2017 | 8039.23 | 11.72 | 0.05 | 11.74 | 0.03 | 11.61 | 0.03 | — | — |
| 13 October 2017 | 8040.27 | 11.83 | 0.04 | 11.84 | 0.02 | 11.69 | 0.02 | — | — |
| 15 October 2017 | 8042.22 | 12.09 | 0.08 | 12.08 | 0.04 | 11.93 | 0.08 | — | — |
| 16 October 2017 | 8043.23 | 12.27 | 0.15 | 12.29 | 0.05 | 12.17 | 0.02 | — | — |
| 17 October 2017 | 8044.22 | 12.57 | 0.04 | 12.51 | 0.02 | 12.33 | 0.02 | — | — |
| 18 October 2017 | 8045.22 | 13.12 | 0.03 | 12.99 | 0.03 | 12.73 | 0.05 | — | — |
| 19 October 2017 | 8046.24 | 13.75 | 0.02 | 13.59 | 0.03 | 13.27 | 0.05 | — | — |
| 20 October 2017 | 8047.21 | 14.15 | 0.09 | 13.75 | 0.02 | 13.37 | 0.05 | — | — |
| 22 October 2017 | 8049.22 | — | — | 14.39 | 0.04 | — | — | — | — |
| 23 October 2017 | 8050.22 | 14.77 | 0.02 | 14.41 | 0.04 | 13.85 | 0.05 | — | — |
| 24 October 2017 | 8051.22 | 14.79 | 0.02 | 14.39 | 0.06 | 13.82 | 0.04 | — | — |
| 25 October 2017 | 8052.23 | 14.34 | 0.17 | 14.31 | 0.05 | 13.78 | 0.01 | — | — |
| 28 October 2017 | 8055.21 | 13.86 | 0.02 | 13.56 | 0.03 | 13.31 | 0.01 | — | — |
| 30 October 2017 | 8057.24 | 12.75 | 0.06 | 12.59 | 0.05 | 12.46 | 0.02 | — | — |
| 01 November 2017 | 8059.24 | 11.79 | 0.07 | 11.83 | 0.02 | 11.73 | 0.02 | — | — |
| 11 November 2017 | 8069.21 | 14.01 | 0.12 | 13.67 | 0.07 | 13.39 | 0.04 | — | — |
| 10 May 2018 | 8249.34 | 14.62 | 0.02 | 14.14 | 0.03 | 13.75 | 0.08 | 13.24 | 0.08 |
| 12 May 2018 | 8251.37 | — | — | 14.01 | 0.03 | — | — | — | — |
| 18 May 2018 | 8257.34 | 12.90 | 0.02 | 12.79 | 0.02 | 12.58 | 0.06 | 12.41 | 0.05 |
| 19 May 2018 | 8258.37 | — | — | 12.39 | 0.02 | — | — | — | — |
| 23 May 2018 | 8262.32 | 12.44 | 0.02 | 12.33 | 0.04 | 12.21 | 0.02 | 12.19 | 0.06 |
| 24 May 2018 | 8263.31 | 12.68 | 0.02 | 12.54 | 0.04 | 12.31 | 0.08 | 12.15 | 0.05 |
| 25 May 2018 | 8264.32 | — | — | 13.71 | 0.06 | — | — | — | — |
| 27 May 2018 | 8266.35 | — | — | 13.69 | 0.04 | 13.14 | 0.16 | — | — |
| 01 June 2018 | 8271.33 | 15.06 | 0.02 | 14.59 | 0.04 | 14.06 | 0.15 | 13.65 | 0.03 |
| 02 June 2018 | 8272.33 | 14.90 | 0.02 | 14.39 | 0.05 | 13.98 | 0.09 | 13.38 | 0.05 |
| 09 June 2018 | 8279.33 | 12.72 | 0.06 | 12.61 | 0.03 | 12.47 | 0.04 | 12.41 | 0.02 |
| 10 June 2018 | 8280.32 | 12.16 | 0.05 | 12.22 | 0.03 | 12.13 | 0.02 | 12.11 | 0.09 |
| 11 June 2018 | 8281.32 | 12.02 | 0.05 | 11.86 | 0.02 | 11.74 | 0.11 | 11.72 | 0.08 |
| 14 June 2018 | 8284.32 | 11.55 | 0.02 | 11.41 | 0.02 | 11.43 | 0.02 | 11.81 | 0.03 |
| 15 June 2018 | 8285.33 | 11.76 | 0.02 | 11.71 | 0.04 | 11.66 | 0.03 | 11.39 | 0.11 |
| 16 June 2018 | 8286.32 | — | — | 11.82 | 0.03 | — | — | — | — |
| 18 June 2018 | 8288.32 | 12.06 | 0.12 | 12.05 | 0.02 | 11.93 | 0.05 | 11.75 | 0.09 |
| 19 June 2018 | 8289.33 | 12.43 | 0.02 | 12.32 | 0.03 | 12.14 | 0.12 | 11.92 | 0.10 |
| 24 June 2018 | 8294.44 | — | — | 13.88 | 0.03 | — | — | — | — |
| 26 June 2018 | 8296.33 | 14.76 | 0.02 | 14.02 | 0.02 | 13.86 | 0.02 | 13.33 | 0.09 |
| 27 June 2018 | 8297.32 | 14.67 | 0.02 | 14.32 | 0.07 | 13.77 | 0.03 | 13.21 | 0.09 |
| 30 June 2018 | 8300.39 | — | — | 14.11 | 0.05 | 13.57 | 0.05 | — | — |
| 01 July 2018 | 8301.34 | 14.44 | 0.02 | 13.96 | 0.05 | 13.51 | 0.05 | 13.05 | 0.11 |

Table continued on following pages

Appendix A: B, V, R_c, I_c observed magnitude data for the dwarf nova AH Her during the years 2012, 2014, 2017, and 2018 (cont).

| <i>Date</i> | <i>JD(2450000.0+)</i> | <i>B</i> | <i>Error</i> | <i>V</i> | <i>Error</i> | <i>R_c</i> | <i>Error</i> | <i>I_c</i> | <i>Error</i> |
|-------------------|-----------------------|----------|--------------|----------|--------------|----------------------|--------------|----------------------|--------------|
| 02 July 2018 | 8302.34 | 14.25 | 0.03 | 13.89 | 0.06 | 13.61 | 0.05 | 13.01 | 0.06 |
| 05 July 2018 | 8305.33 | — | — | 14.32 | 0.04 | — | — | 13.22 | 0.02 |
| 06 July 2018 | 8306.34 | 15.06 | 0.02 | 14.43 | 0.02 | — | — | 13.32 | 0.03 |
| 07 July 2018 | 8307.35 | 15.03 | 0.03 | 14.44 | 0.02 | — | — | 13.36 | 0.06 |
| 08 July 2018 | 8308.34 | 14.98 | 0.06 | 14.38 | 0.02 | — | — | 13.46 | 0.02 |
| 09 July 2018 | 8309.33 | 13.73 | 0.06 | 13.55 | 0.02 | — | — | 12.89 | 0.02 |
| 10 July 2018 | 8310.36 | 13.01 | 0.04 | 12.93 | 0.03 | — | — | 12.61 | 0.05 |
| 11 July 2018 | 8311.35 | 12.45 | 0.04 | 12.38 | 0.04 | — | — | 12.11 | 0.03 |
| 13 July 2018 | 8313.32 | 12.16 | 0.05 | 11.73 | 0.04 | — | — | 11.49 | 0.02 |
| 14 July 2018 | 8314.38 | — | — | 11.66 | 0.02 | — | — | — | — |
| 15 July 2018 | 8315.33 | 11.78 | 0.02 | 11.82 | 0.02 | — | — | 11.51 | 0.03 |
| 17 July 2018 | 8317.32 | 12.01 | 0.03 | 11.89 | 0.07 | — | — | 11.41 | 0.12 |
| 18 July 2018 | 8318.33 | — | — | 12.19 | 0.06 | — | — | — | — |
| 19 July 2018 | 8319.30 | 12.37 | 0.05 | 12.38 | 0.02 | — | — | 12.06 | 0.18 |
| 20 July 2018 | 8320.33 | 13.11 | 0.05 | 12.89 | 0.02 | — | — | 12.52 | 0.05 |
| 21 July 2018 | 8321.38 | — | — | 13.28 | 0.02 | 12.89 | 0.03 | — | — |
| 23 July 2018 | 8323.32 | 14.47 | 0.03 | 14.16 | 0.05 | — | — | 13.63 | 0.11 |
| 24 July 2018 | 8324.31 | 14.62 | 0.02 | 14.18 | 0.04 | — | — | 13.11 | 0.03 |
| 25 July 2018 | 8325.31 | 14.52 | 0.03 | 14.26 | 0.09 | — | — | 13.32 | 0.11 |
| 29 July 2018 | 8329.31 | 14.31 | 0.05 | 13.93 | 0.10 | — | — | 13.05 | 0.02 |
| 31 July 2018 | 8331.32 | 14.75 | 0.02 | 14.14 | 0.03 | — | — | 13.27 | 0.08 |
| 01 August 2018 | 8332.30 | 14.66 | 0.02 | 14.01 | 0.11 | — | — | 12.94 | 0.07 |
| 02 August 2018 | 8333.32 | 14.41 | 0.01 | 14.03 | 0.04 | — | — | 13.24 | 0.02 |
| 03 August 2018 | 8334.32 | 13.45 | 0.02 | 13.13 | 0.06 | — | — | 12.69 | 0.04 |
| 04 August 2018 | 8335.35 | — | — | 12.59 | 0.04 | 12.47 | 0.01 | — | — |
| 05 August 2018 | 8336.31 | 12.07 | 0.03 | 11.98 | 0.01 | — | — | 11.76 | 0.03 |
| 09 August 2018 | 8340.34 | 12.27 | 0.03 | 12.14 | 0.04 | — | — | 11.84 | 0.02 |
| 10 August 2018 | 8341.34 | — | — | 12.28 | 0.02 | 12.11 | 0.02 | — | — |
| 16 August 2018 | 8347.31 | 14.34 | 0.04 | 13.97 | 0.06 | — | — | 13.02 | 0.10 |
| 17 August 2018 | 8348.36 | — | — | 13.81 | 0.03 | 13.41 | 0.02 | — | — |
| 19 August 2018 | 8350.30 | 14.37 | 0.02 | 14.01 | 0.04 | — | — | 13.28 | 0.02 |
| 20 August 2018 | 8351.30 | — | — | 14.14 | 0.06 | — | — | 13.10 | 0.05 |
| 21 August 2018 | 8352.33 | — | — | 13.94 | 0.02 | — | — | — | — |
| 22 August 2018 | 8353.30 | 14.46 | 0.03 | 14.01 | 0.03 | — | — | 13.30 | 0.06 |
| 23 August 2018 | 8354.30 | 14.28 | 0.07 | 13.90 | 0.02 | — | — | — | — |
| 24 August 2018 | 8355.32 | 14.65 | 0.10 | 14.16 | 0.02 | — | — | 13.17 | 0.06 |
| 25 August 2018 | 8356.34 | — | — | 14.04 | 0.09 | 13.43 | 0.04 | — | — |
| 26 August 2018 | 8357.29 | 14.28 | 0.07 | 12.99 | 0.04 | — | — | 12.53 | 0.08 |
| 27 August 2018 | 8358.28 | 11.88 | 0.03 | 11.91 | 0.03 | — | — | 11.69 | 0.05 |
| 28 August 2018 | 8359.28 | 11.91 | 0.05 | 11.87 | 0.02 | — | — | — | — |
| 28 August 2018 | 8359.30 | 11.75 | 0.05 | — | — | — | — | — | — |
| 29 August 2018 | 8360.30 | 11.71 | 0.05 | 11.72 | 0.03 | — | — | 11.36 | 0.07 |
| 30 August 2018 | 8361.34 | 11.69 | 0.04 | 11.61 | 0.02 | — | — | 11.17 | 0.15 |
| 01 September 2018 | 8363.28 | 12.07 | 0.04 | 12.02 | 0.03 | — | — | 11.73 | 0.03 |
| 02 September 2018 | 8364.29 | 12.12 | 0.02 | 12.09 | 0.02 | 11.93 | 0.01 | 11.78 | 0.03 |
| 03 September 2018 | 8365.30 | 12.38 | 0.02 | 12.25 | 0.05 | 12.09 | 0.06 | 11.99 | 0.06 |
| 05 September 2018 | 8367.27 | 13.37 | 0.05 | 13.21 | 0.03 | 12.97 | 0.02 | 12.63 | 0.04 |
| 08 September 2018 | 8370.26 | 14.63 | 0.09 | 14.22 | 0.02 | 13.78 | 0.01 | 13.17 | 0.04 |
| 09 September 2018 | 8371.29 | 14.64 | 0.01 | 14.25 | 0.02 | 13.81 | 0.02 | 13.32 | 0.06 |
| 10 September 2018 | 8372.27 | 15.04 | 0.08 | 14.51 | 0.06 | 14.10 | 0.01 | 13.45 | 0.06 |
| 11 September 2018 | 8373.26 | 14.81 | 0.02 | 14.56 | 0.03 | 13.89 | 0.04 | 13.49 | 0.01 |
| 12 September 2018 | 8374.27 | 14.78 | 0.02 | 14.28 | 0.02 | 13.86 | 0.01 | 13.26 | 0.02 |
| 22 September 2018 | 8384.26 | 12.17 | 0.03 | 12.17 | 0.07 | 11.96 | 0.05 | 11.84 | 0.02 |
| 23 September 2018 | 8385.26 | 12.44 | 0.02 | 12.28 | 0.02 | 12.09 | 0.03 | 11.97 | 0.05 |
| 26 September 2018 | 8388.26 | 13.54 | 0.05 | 13.41 | 0.01 | 13.07 | 0.02 | 12.83 | 0.04 |
| 27 September 2018 | 8389.28 | 14.02 | 0.02 | 13.77 | 0.04 | 13.43 | 0.02 | 13.08 | 0.08 |
| 28 September 2018 | 8390.25 | 14.61 | 0.02 | 14.14 | 0.03 | 13.71 | 0.03 | 13.04 | 0.01 |
| 29 September 2018 | 8391.32 | — | — | 14.15 | 0.03 | — | — | — | — |
| 30 September 2018 | 8392.26 | — | — | 14.51 | 0.03 | — | — | — | — |
| 02 October 2018 | 8394.31 | 14.91 | 0.07 | 14.54 | 0.02 | 14.09 | 0.02 | 13.46 | 0.08 |
| 03 October 2018 | 8395.23 | 14.69 | 0.01 | 14.18 | 0.10 | 13.88 | 0.06 | 13.44 | 0.08 |
| 07 October 2018 | 8399.27 | 14.71 | 0.05 | 14.17 | 0.11 | 13.79 | 0.02 | 13.31 | 0.05 |
| 08 October 2018 | 8400.24 | 14.66 | 0.06 | 14.24 | 0.06 | 13.87 | 0.10 | 13.42 | 0.05 |
| 12 October 2018 | 8404.25 | 12.13 | 0.03 | 12.06 | 0.02 | 11.96 | 0.03 | 11.91 | 0.04 |
| 13 October 2018 | 8405.23 | 11.68 | 0.03 | 11.69 | 0.02 | 11.55 | 0.02 | 11.51 | 0.02 |
| 19 October 2018 | 8411.23 | 12.18 | 0.03 | 12.10 | 0.04 | 11.97 | 0.03 | 11.87 | 0.02 |
| 20 October 2018 | 8412.21 | 13.37 | 0.03 | 12.28 | 0.08 | — | — | 12.11 | 0.02 |
| 22 October 2018 | 8414.24 | 13.33 | 0.05 | 13.05 | 0.05 | 12.85 | 0.06 | 12.71 | 0.07 |

Table continued on next page

Appendix A: B, V, R_c, I_c observed magnitude data for the dwarf nova AH Her during the years 2012, 2014, 2017, and 2018 (cont).

| <i>Date</i> | <i>JD(2450000.0+)</i> | <i>B</i> | <i>Error</i> | <i>V</i> | <i>Error</i> | <i>R_c</i> | <i>Error</i> | <i>I_c</i> | <i>Error</i> |
|------------------|-----------------------|----------|--------------|----------|--------------|----------------------|--------------|----------------------|--------------|
| 23 October 2018 | 8415.23 | 13.64 | 0.05 | 13.49 | 0.04 | 13.19 | 0.05 | 12.84 | 0.04 |
| 24 October 2018 | 8416.24 | 13.86 | 0.02 | 13.57 | 0.02 | 13.31 | 0.03 | 12.97 | 0.02 |
| 25 October 2018 | 8417.24 | 13.91 | 0.08 | 13.55 | 0.04 | 13.22 | 0.02 | 12.76 | 0.06 |
| 08 November 2018 | 8431.25 | 14.42 | 0.04 | 14.02 | 0.02 | 13.68 | 0.02 | 13.31 | 0.03 |
| 09 November 2018 | 8432.26 | 14.53 | 0.07 | 14.31 | 0.06 | 13.79 | 0.02 | 13.29 | 0.04 |
| 10 November 2018 | 8433.21 | 14.76 | 0.01 | 14.22 | 0.04 | 13.71 | 0.02 | 13.19 | 0.05 |
| 11 November 2018 | 8434.20 | 14.74 | 0.09 | 14.19 | 0.02 | 13.74 | 0.03 | 13.34 | 0.04 |
| 15 November 2018 | 8438.23 | 13.54 | 0.08 | 13.27 | 0.02 | 13.04 | 0.02 | 12.91 | 0.07 |
| 16 November 2018 | 8439.22 | 13.23 | 0.07 | 12.98 | 0.05 | 13.45 | 0.05 | 12.69 | 0.05 |
| 17 November 2018 | 8440.23 | 12.88 | 0.04 | — | — | — | — | 12.42 | 0.03 |
| 18 November 2018 | 8441.19 | 12.36 | 0.10 | 12.41 | 0.05 | 12.17 | 0.12 | 12.13 | 0.12 |
| 01 December 2018 | 8454.19 | 14.26 | 0.19 | 13.88 | 0.03 | 13.43 | 0.05 | 13.18 | 0.05 |